

The Rise of Bacterial G-Quadruplexes in Current Antimicrobial Discovery

Stefano Ciaco, Rossella Aronne, Martina Fiabane, and Mattia Mori*



Cite This: *ACS Omega* 2024, 9, 24163–24180



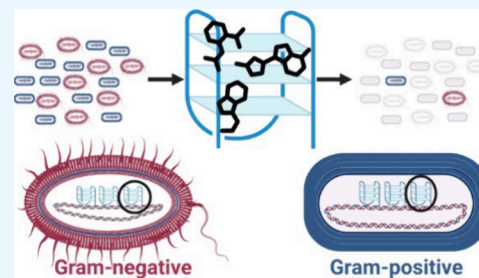
Read Online

ACCESS |

Metrics & More

Article Recommendations

ABSTRACT: Antimicrobial resistance (AMR) is a silent critical issue that poses several challenges to health systems. While the discovery of novel antibiotics is currently stalled and prevalently focused on chemical variations of the scaffolds of available drugs, novel targets and innovative strategies are urgently needed to face this global threat. In this context, bacterial G-quadruplexes (G4s) are emerging as timely and profitable targets for the design and development of antimicrobial agents. Indeed, they are expressed in regulatory regions of bacterial genomes, and their modulation has been observed to provide antimicrobial effects with translational perspectives in the context of AMR. In this work, we review the current knowledge of bacterial G4s as well as their modulation by small molecules, including tools and techniques suitable for these investigations. Finally, we critically analyze the needs and future directions in the field, with a focus on the development of small molecules as bacterial G4s modulators endowed with remarkable drug-likeness.



1. INTRODUCTION

The World Health Organization (WHO) has identified antimicrobial resistance (AMR) as one of the top three health threats of the 21st century and recently published a priority list of drug- or multidrug-resistant (MDR) bacteria for which new antibiotics are urgently needed, including Gram-positive and Gram-negative species.^{1,2} Six of them are also included in a group of highly virulent AMR pathogens that is commonly classified with the acronym ESKAPE, which includes *Enterococcus faecium*, *Staphylococcus aureus*, *Klebsiella pneumoniae*, *Acinetobacter baumannii*, *Pseudomonas aeruginosa*, and *Enterobacter spp.*³ The lack of effective therapeutic options against ESKAPE bacteria has seriously increased the burden of bacterial diseases and the death rate in infected patients, with the concrete risk of bacteria spreading outside clinical settings where they are commonly found. It has been recently estimated that the uncontrolled spread of drug-resistant bacteria could lead to more than 10 million deaths worldwide by 2050.⁴

Besides a few virtuous examples such as human immunodeficiency virus-1 (HIV-1) and the hepatitis-C virus (HCV) for which effective therapeutics have been developed,^{5,6} in the last few decades, drug development efforts toward infectious diseases have been rare, especially compared to those for cancer and metabolic disorders. Bacterial infections represent a concrete health threat worldwide, with the potential to become one of the major causes of death in a few years.⁷ This scenario might become real or even worse if new antibiotics, preferably endowed with innovative mechanisms of action, are not developed in the incoming years. Indeed, following the peak of antibiotics recorded in the 60s

and 70s, in the last few decades, breakthroughs in this field have seriously declined.⁸ Most of the so-named “new” antibiotics merely incorporate slight modifications to validate the chemical scaffolds of existing drugs, becoming ineffective at escaping the drug resistance mechanisms already acquired by the pathogens. Moreover, bacteria have rapidly developed resistance to these chemical classes, generating a plethora of pandrug-resistant (PDR) strains, which are often referred to as superbugs. In this critical situation, it is worth noting that the spread of AMR is accelerated by the massive use and misuse of antibiotics for prolonged prophylaxis therapies, inappropriate self-medication, food-producing animal prophylaxis, and uncontrolled release of antibiotics in wastewaters.^{9–11}

The recent COVID-19 pandemic has highlighted the lack of time- and cost-effective strategies to face the outbreaks of new pathogens. Extraordinary worldwide efforts have been spent to develop/repurpose drugs^{12–14} and to develop innovative RNA-based vaccines.^{15,16} Remarkably, these progresses have been strongly boosted by massive structural biology efforts,^{17–19} which are unfortunately unprecedented and not yet exploited in the study of other pathogens that currently impair human health, such as bacteria.

Received: February 22, 2024

Revised: May 10, 2024

Accepted: May 17, 2024

Published: May 30, 2024



A recent report of the Centers for Disease Control and Prevention (CDC) has also linked AMR spread to the COVID-19 pandemic as a consequence of the increased and unmotivated use of antibiotics. Considering data retrieved from the United States of America (USA) health systems, around 80% of hospitalized COVID-19 patients received an antibiotic in the period from March 2020 to October 2020²⁰ as prophylaxis or self-medication, although being irrational and ineffective. This has led to a growth of infections by drug-resistant pathogens, with an impressive increase of at least 15% provided by Carbapenem-resistant *Acinetobacter* (+78%).²¹

Overall, the WHO has underlined the criticisms and risks associated with the current AMR scenario, highlighting the need for alternative and innovative therapeutic solutions with a strong focus on both AMR and the potential emergence of novel pathogens or novel strains of existing pathogens. The lack of effective antibacterial drugs points to the urgency in identifying novel chemical classes or novel targets, with a specific emphasis on those macromolecules that are crucial for the survival of the bacteria but are endowed with a low susceptibility to mutation in response to pharmacological pressure. Moreover, in an emergency-like scenario, the ideal target should be easily and rapidly identifiable to allow for fast access to drug design or repurposing campaigns. While three-dimensional structures of human targets, such as proteins and nucleic acids, have been extensively characterized,^{22,23} microbial targets remain poorly investigated, with only a few exceptions (e.g., HIV-1 reverse transcriptase, bacterial β -lactamases, polymerases, etc.).^{24–27} This highlights the need to fill this knowledge gap, with the aim to promote concerted and multidisciplinary actions that are focused to the rational development of innovative antimicrobial candidates.^{28–30}

In a traditional scenario, proteins are mainly perceived as the ideal target of therapeutically relevant small molecules such as drug candidates, which can be designed based on the shape and chemical composition of the target's binding site. However, the characterization of the three-dimensional structures of proteins for drug and vaccine design studies remains a time- and cost-demanding procedure. Indeed, several steps such as cloning, expression, purification, and structural biology studies are needed before atomistic details might be eventually available. Although many efforts are being devoted to the generation of reliable models of yet unknown proteins structures through homology modeling, metagenomic data, contact-based structure matching, and methods based on artificial intelligence (AI) such as AlphaFold, these prediction tools have some limitations and experimental validation might be required, especially from a drug discovery perspective.^{31–35}

In contrast, considering the strong evolution of sequencing methods, including next generation sequencing (NGS) technologies, genomic sequences of emerging or spreading pathogens are becoming rapidly available after the isolation of the pathogen.^{36–38} Access to sequence and structural features of nucleic acids might occur with relatively fewer efforts and less time compared to protein structural elucidation. Consequently, specific nucleic acid regions, such as promoter sequences, *cis*-regulatory elements, conserved noncoding elements (CNEs), etc., are emerging as profitable targets in drug design.^{39,40}

Among nucleic acid structures, in the last few decades particular attention has been dedicated to G-quadruplexes (G4s), i.e., noncanonical DNA and/or RNA structural motifs that form in guanine-rich sequences.^{41,42} G4s have been widely

investigated as anticancer targets due to their presence in telomeres and oncogene promoters.^{43,44} Moreover, the few available reports on the potential application of G4s as drug delivery systems or as the main component of supramolecular hydrogels have been reviewed.^{45,46} In recent years, the study of G4s as potential targets for antimicrobial therapy has grown,^{47,48} which prompted us to summarize herein the available knowledge on bacterial G4s and their potential modulation/stabilization by small molecules. In this Review, the structural and functional features of G4s are overviewed, with a specific focus on the knowledge available on bacterial G4s, including preliminary attempts to target these structures with known G4s binders.

2. MAIN STRUCTURAL FEATURES OF G4S

Although the structural features of G4s have been deeply reviewed elsewhere,^{49–51} here we provide a general overview of G4s structures and summarize the structural details available for bacterial G4s.

The main structural unit of a G4 is a quartet of coplanar guanine nucleotides (often referred to as a G-quartet or G-tetrad, Figure 1A) tightly held together by Hoogsteen hydrogen bonds. Based on the dihedral angle (χ) between the sugar and the base, the guanine residue in a G-tetrad can adopt two different configurations: (i) *anti* and (ii) *syn*, which occur when χ lies in the 180°–240° and 0°–90° ranges, respectively.

Potential G4-forming sequences have been found in several organisms, such as vertebrates (evolutionary close to *Homo sapiens*), and yeasts (e.g., *Saccharomyces cerevisiae*), viruses (e.g., HIV-1), parasites (e.g., *Plasmodium falciparum*), and bacteria (e.g., *Escherichia coli*), suggesting that G4s are highly evolutionarily conserved through functional parts of different and distant genomes.^{52–54} In canonical G4s, at least two G-quartets stack on top of each other, connected by four strands that might derive from a single or multiple nucleic acid molecules. The stacking of two or more G-tetrads on the top of each other creates a negatively charged cavity in the inner part of a folded G4, which can accommodate monovalent metal ions (mostly K⁺ or Na⁺, although other cations can be hosted)⁵⁵ through coordination by the O6 atoms of guanine bases from the G-tetrads (Figure 1A). Given the variability of the atomic radius and mobility of monovalent ions that are known to coordinate the guanine bases within the inner cavity of stacked G-tetrads, differential stabilization effects are provided. While K⁺ seems to have ideal coordination features, being located 2.73 Å from eight O6 atoms and providing the strongest G4 stabilization effect, Na⁺ can preferentially bind in the middle of a G-quartet or slightly above/below the plane of a folded G-tetrad, providing a weaker stabilization of the G4 than K⁺.^{56,57} For this reason, K⁺ is the cation most commonly used in structural investigations of G4s.^{55,58}

Three-dimensional structures of G4s have been characterized by X-ray crystallography and nuclear magnetic resonance (NMR) spectroscopy, showing that most of them are formed by intramolecular folds or by the connection of strands from two different nucleic acid molecules. Nevertheless, G4s formed by three or four separated strands are rare but possible. Different topologies have also been identified: parallel, antiparallel, and hybrid, in function of the relative 5'-3' direction of the four strands (Figure 1B–D), with the parallel topology being dominant in human RNA G4s and bacterial G4s.^{59–62}

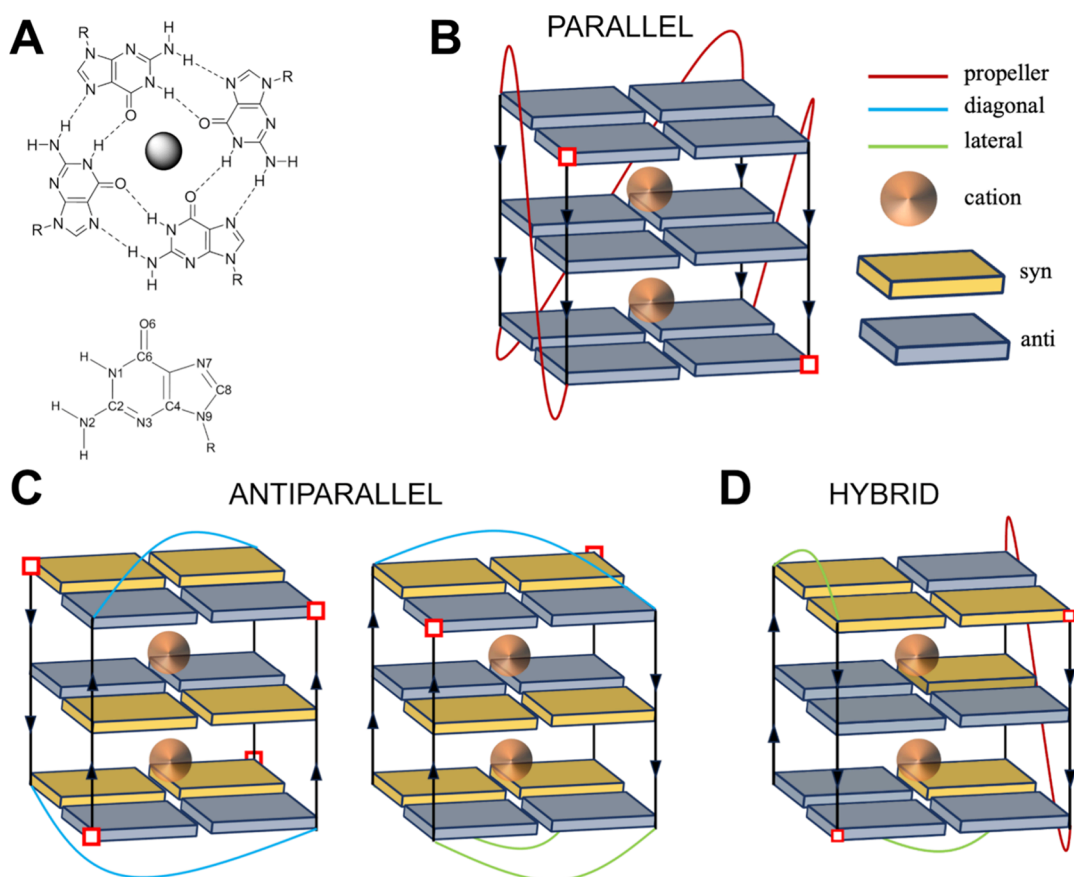


Figure 1. Structural features of the G4s. (A) Chemical depiction of a G-tetrad with a cation in its inner part (gray sphere) (top). Hoogsteen hydrogen bonds are represented as dashed lines. Chemical structure of the guanine base with atom names (bottom). (B) Schematic representation of a parallel G4; propeller loops are colored red. (C) Schematic representation of antiparallel G4s; lateral loops are colored green, and diagonal loops are colored cyan. (D) Schematic representation of a hybrid G4; loops are colored as in B and C. The cation is shown as an orange sphere, guanine in the *syn* conformation is shown as a yellow box, and guanine in the *anti* conformation is shown as a gray box. 5' and 3' terminals are represented as red squares. Adapted from Largy et al.⁵⁵

The loops connecting the G-quartets represent the most variable portion of G4s and may influence their structure and topology. Among different G4s, loops differ in terms of length and nucleobase composition, and they can be classified into four major groups (Figure 1): (i) diagonal loops connect two adjacent G-tetrads diagonally across the G4 structure; (ii) lateral loops (also referred as edgewise loops) occur at the edges of G-tetrads, where one or more nucleotides extend outward the G-tetrad core; (iii) propeller loops (also referred as chain-reversal loops) are characterized by a propeller-like rotation of bases around the loop leading to extensive base stacking interactions within the loop region, where the reversal can involve one or more (double or triple chain-reversal) nucleic acid strands; and (iv) V-shaped loops in which the nucleic acid backbone folds back on itself, forming a structure resembling the letter “V” (not highlighted in Figure 1). Noteworthy, mixed-loop configurations can occur, displaying a combination of different types of loops within the same loop region.^{63,64} The spaces between the four strands are termed grooves; in contrast with canonical DNA and RNA duplexes, G4s have four grooves, whose dimensions depend on the G4 topology and on the size and sequence of the loops.

Several structural studies have characterized the tertiary structure of more than 350 G4s, which are available in the Protein Data Bank or Nucleic Acid Database (PDB and NDB, respectively).^{22,23} The majority of these structures are from

human sequences or synthetic constructs, whereas a very limited subset are characterized by bacterial G4 structures. According to a search carried out in the PDB in December 2023, only two G4s structures from bacterial origin have been solved, i.e., the *pileE* DNA G4 from *Neisseria gonorrhoeae* in its monomeric (PDB ID 2LXQ) and dimeric forms (PDB ID 2LXV) as characterized by NMR spectroscopy (Figure 2).⁶⁵

Although we are aware that this search might have lost a few bacterial G4 structures, this result highlights the structural limitations in investigating G4s from species that differ from those of *Homo sapiens*. Anyway, this should not be discouraging, since the restricted alphabet of nucleic acids has permitted some short sequences to be shared by multiple organisms, and some synthetic constructs might correspond to sequences expressed in bacteria or in other pathogens. Notably, some of these sequences have been characterized by X-ray crystallography or NMR spectroscopy, granting access to precious structural information on bacterial DNA sequences that fold as G4s. A notable example is represented by TET22, a G4 expressed in *Pseudomonas aeruginosa*, whose structure is not explicitly solved by structural biology approaches. However, its $(T_2G_4)_4$ sequence fully overlaps with the sequence of a telomeric G4 characterized in the protozoa *Tetrahymena*, for which the structure has been solved by NMR spectroscopy.⁶⁶

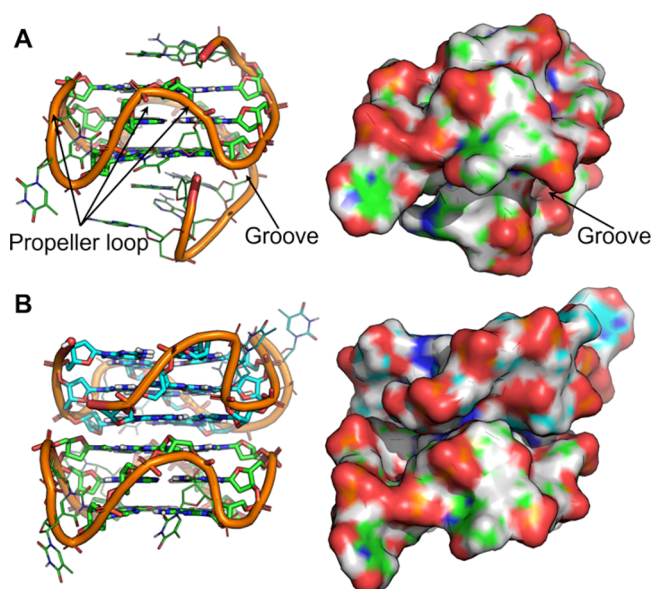


Figure 2. Experimental structures of bacterial G4s found in the PDB. NMR structures of (A) monomeric and (B) dimeric pilE G4 from *N. gonorrhoeae* (PDB IDs 2LXQ and 2LXV, respectively).⁶⁵ Left panels: cartoon representation of G4s. Guanine forming the G-tetrad are shown as sticks, and other nucleotides are shown as lines. Right panels: surface representation of G4s. The two monomeric units of pilE in the dimeric form are colored green and cyan, respectively.

Structural and biophysical studies (see section 3) on G4s have been largely conducted on specific oligonucleotide sequences cut at the 5' and 3' ends, which fail to describe a physiological scenario. In fact, G4s are generally expressed in long genome sequences, with dangling nucleotides at both ends. Some of these dangling ends have been also characterized in human G4s, showing interaction with G-tetrads.^{67,68} The influence of dangling nucleotides at the 5' end has been observed in the human Tel22 G4, indicating that the addition of single-stranded sequences at the 5' end may impact the loop geometry and unfolding thermodynamics through entropic and enthalpic effects, which are mostly due to the interaction of dangling nucleotides with the terminal G-tetrad as well as the displacement of water molecules.⁶⁹ These findings have been also corroborated by coupling the dangling 5' end with a fluorophore moiety, clearly indicating that stacking to the terminal G-tetrad may influence G4s topology.⁷⁰

Structure prediction tools such as homology modeling and AlphaFold fail to work with nucleic acids structural templates. Nevertheless, some attempts to predict the structure of a G4 by coupling spectroscopic data (see below) with the structures of relatively similar sequences have been carried out.^{71–73} Anyway, the availability of bacterial G4s structures still represents a major drawback in G4-oriented drug design.

3. IDENTIFICATION OF G4S AND THEIR BIOPHYSICAL PROPERTIES

In the last few decades, a series of bioinformatics tools have been developed to identify putative G4s in target genomes by exploiting peculiar features such as G-richness, loop lengths, and specific patterns in loop and in flanking sequences. Among them, Quadparser, G4 calculator, QGRS Mapper, G4Hunter, and QuadBase have been developed and extensively tested.^{74–77} Most of them use a consensus algorithm sequences, i.e. $G_{3+N_{1-7}G_{3+N_{1-7}G_{3+N_{1-7}G_{3+}}$, resulting in more than 350 000 putative G4 sequences.⁵² However, these putative sequences may not fold into a structured and stable G4, and G4s that fail to match these common sequence patterns cannot be identified, which suggests that the consensus algorithm might be endowed with intrinsic limitations in the effective search of G4 sequences within genomes of parts of them.⁵² Confirmation that a putative G4 sequence effectively folds into a stable G4 is usually achieved by combining bioinformatics approaches with a plethora of biophysical techniques, including UV spectroscopy, fluorescent-based approaches such as Förster resonance energy transfer (FRET), anisotropy and quenching approaches, circular dichroism (CD), and structural biology methods such as X-ray crystallography and NMR spectroscopy.^{78–80}

G4s are stable under physiological conditions but unfold at high temperatures (usually above 60 °C). Model oligonucleotides used for biophysical assays exhibit lower thermal stability (50–60 °C) than their duplex counter parts (>60 °C) in similar biophysical experimental conditions. The melting temperature (T_m) of G4s can widely vary depending on factors such as the sequence, cation type, and concentration, as well as the presence of ligands, allowing a wide temperature range of 60–95 °C to quantify the thermal stabilization provided by G4-stabilizing ligands. Moreover, the annealing of a typical DNA double helix is accompanied by a decrease in the absorbance at ~260 nm (hypochromism), whereas the formation of a Hoogsteen base pairing such as typical in G-tetrads (Figure 1A) is accompanied by an increase in

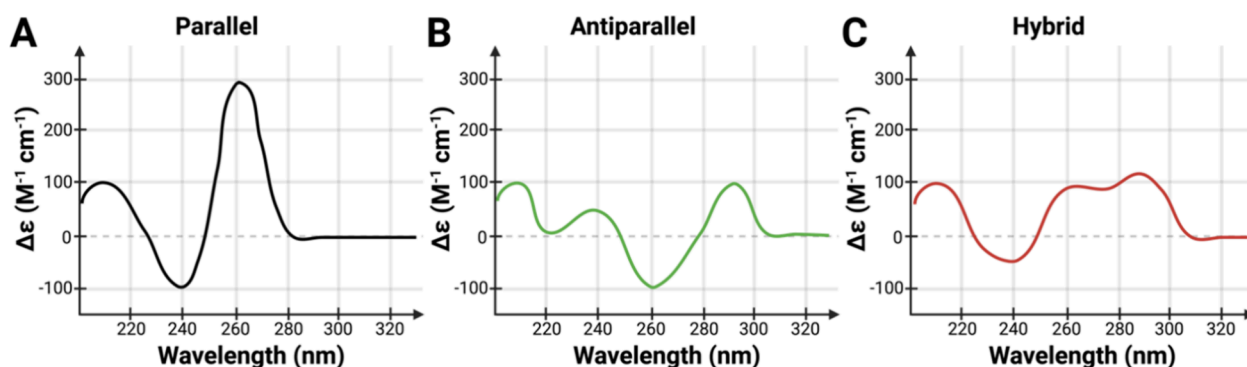


Figure 3. Putative CD spectra of G4s depending on their topology: (A) CD spectrum of a parallel G4, (B) CD spectrum of an antiparallel G4, and (C) CD spectrum of a hybrid G4. CD spectra have been designed based on literature data and created with BioRender.com.

absorbance at ~ 295 nm and a decrease at ~ 260 nm, rendering UV spectroscopy a suitable method to monitor G4 folding and discriminate G4s from DNA duplexes.^{81,82} Nevertheless, information on strand segment orientation, loop arrangements, and topology of G4s is not accessible by UV but can be provided by CD spectroscopy.

The CD signature of parallel G4s (Figure 3A) is characterized by a positive peak at ~ 264 nm and a negative peak at ~ 245 nm,⁷¹ whereas a positive maximum peak at ~ 295 nm and a negative minimum peak at ~ 260 nm are diagnostic of antiparallel G4s (Figure 3B) in CD spectra. The CD spectrum of an antiparallel G4 shows two additional smaller peaks at ~ 240 and ~ 210 nm. However, CD fails to discriminate the molecularity of G4s, namely *anti-syn-anti-syn* or *anti-anti-syn-syn* conformations of guanine nucleotides forming the G-tetrads. Hybrid G4s (Figure 3C) are characterized by a hybrid CD spectrum, showing a double positive peak at ~ 295 nm with a shoulder or band at around ~ 260 nm, a negative peak at 240 nm, and another positive peak at ~ 210 nm.⁴¹

Additional qualitative information can be obtained using fluorescence-based approaches disclosing accurate information on conformational rearrangements, loop fluctuations, topology, and ligand-binding properties. These can be achieved by exploiting the intrinsic fluorescence of G4s, which can also be used to discriminate G4s from other DNA folding structures,^{68,83–87} as well as by incorporating fluorescent probes into strategic G4 sequence positions.^{88,89} Effective fluorescent purine probes for studying nucleic acids have been developed.⁸⁸ These include (i) 2-aminopurine (2AP), which has been employed to monitor the G4 conformational switch;^{90–92} (ii) 8-vinylguanine (8vG), which can adopt both *syn* and *anti* conformations,⁹³ becoming highly useful in monitoring different G4 topologies; and (iii) thienoguanosine (thG) and isothiazolguanosine (^{tz}G). Although thG and ^{tz}G are isomorphous fluorescent G mimetics that have proven very useful in depicting structural features of double stranded and protein-bound DNA sequences,^{94–100} they have been not exploited yet in G4s. Similarly, isomorphous fluorescent pyrimidine probes ^{SE}dU and ^{FU}dU bearing heteroaryl expansion display a characteristic fluorescence emission pattern that helps to distinguish different folding architectures of nucleic acid, becoming valuable candidates for the study of G4s topologies.^{101,102} Topology and inner cation coordination are also known to influence the excited states and photoionization properties of G4s, which can be investigated through experimental and computational studies.^{103–105} Finally, G4s in living organisms can be detected by the use of specific antibodies^{106,107} that can be eventually conjugated to fluorescent probes^{108,109} and by the use of small molecular probes.^{110,111}

4. ROLE OF G4S IN BACTERIA AND THEIR MODULATION BY SMALL MOLECULES

The therapeutic relevance of human and eukaryotic G4s has been largely addressed up to clinical trials (i.e., **CX-3543**, Cylene Pharmaceuticals), **CX-5461** (Canadian Cancer Trials Group), and **QN-302** (Qualigen Therapeutics, Inc.), (Figure 4A).^{112–116} In contrast, the interest in bacterial G4s was raised later and with less intensity than human G4s, leaving the therapeutic exploitation of bacterial G4s still mostly unexplored. This is also clearly highlighted by an updated interrogation of scientific literature databases such as PubMed

(Figure 4B). Notwithstanding, several lines of evidence link the expression of G4s in pathogenic bacteria and biofilm to their replication, infection, and survival mechanisms, suggesting that targeting bacterial G4s might be an effective strategy in the current discovery of antibiotics.

Most notable findings that highlight the role and relevance of G4s in pathogenic bacteria, as well as preliminary G4 stabilization studies by small molecules, are overviewed below.

4.1. *Escherichia coli*. *E. coli* is a Gram-negative bacterium normally present in the lower intestine of warm-blooded organisms,¹¹⁷ although some virulent strains are responsible for food poisoning and food contamination.¹¹⁸

An enrichment of G4 putative motifs was identified in regulatory regions of several endogenous proteins of *E. coli*, such as RuvA, FIS, Lrp, and the σ -factor RpoD (σ^{70}) that control more than 1000 genes. Through genome-wide approaches, it has been hypothesized that these putative G4s may modulate a wide range of cellular processes. Noteworthy, the G4 motifs are highly conserved among the orthologous genes across phylogenetically distant organisms.¹¹⁷ Moreover, comparative functional analysis of more than 60 000 open reading frames (ORFs) of *E. coli* suggested that transcription, amino acids biosynthesis, and signal transduction genes could be mainly controlled by G4s. Further studies have investigated the effect of the position of G4 sequences in *E. coli* (XL10 gold strain) by combining cloning methods and CD measurements, showing that G4s are preferentially located before the operons rather than between them. This has suggested a regulatory role for G4s in *E. coli*.¹¹⁹ More than 30 operons are in *E. coli* have motif-induced supercoiling sensitivity, supporting a context-dependent gene regulation.¹¹⁷

E. coli has been recently used as a model system in the evaluation of the G4 stabilizing activity by a series of naphthalene diimides (NDIs), a profitable family of electron-deficient and flat molecules that have been thoroughly exploited in several fields including supramolecular and material chemistry, especially within the last two decades.^{120–122} Among the various applications of NDIs, of particular interest for this Review is their capability to stack on the top of electron-rich G-quartets in DNA G4s.¹²³ The development of an effective and flexible synthetic protocol has further allowed for easy chemical modification toward drug-likeness,¹²⁴ such as that underlined by the phase I clinical trial running with **QN-302** (Figure 4, ClinicalTrials.gov ID NCT06086522).¹²⁵

Two putative G4-forming sequences have been identified in the *E. coli* genome (strain LMG8223) using the G4-iM Grinder bioinformatics tool¹²⁶ by Cebrian et al.¹²⁴ The propensity of these sequences (i.e., EC-6 and EC-9, Table 1) to form G4s was confirmed by CD spectra recorded in the presence of 100 mM K⁺, which showed a predominant parallel topology with a maximum peak at ~ 264 nm and a minimum peak at ~ 240 nm. The stabilizing effect of the most promising hit **NDI-10** (Figure 5) was confirmed by FRET melting and CD melting assays, showing a remarkable stabilization of the tested sequences by the small molecule. Notably, **NDI-10** has shown significant antibacterial activity, with a minimum inhibitory concentration (MIC) of 8 μ M against *E. coli*, and also exhibited dose-dependent bactericidal activity with no cell lysis effects. Finally, of the 4930 annotated genes in *E. coli*, 1527 have demonstrated altered expression following treatment with **NDI-10**, with most of them being downregulated. As such, **NDI-10** has been suggested to repress the expression

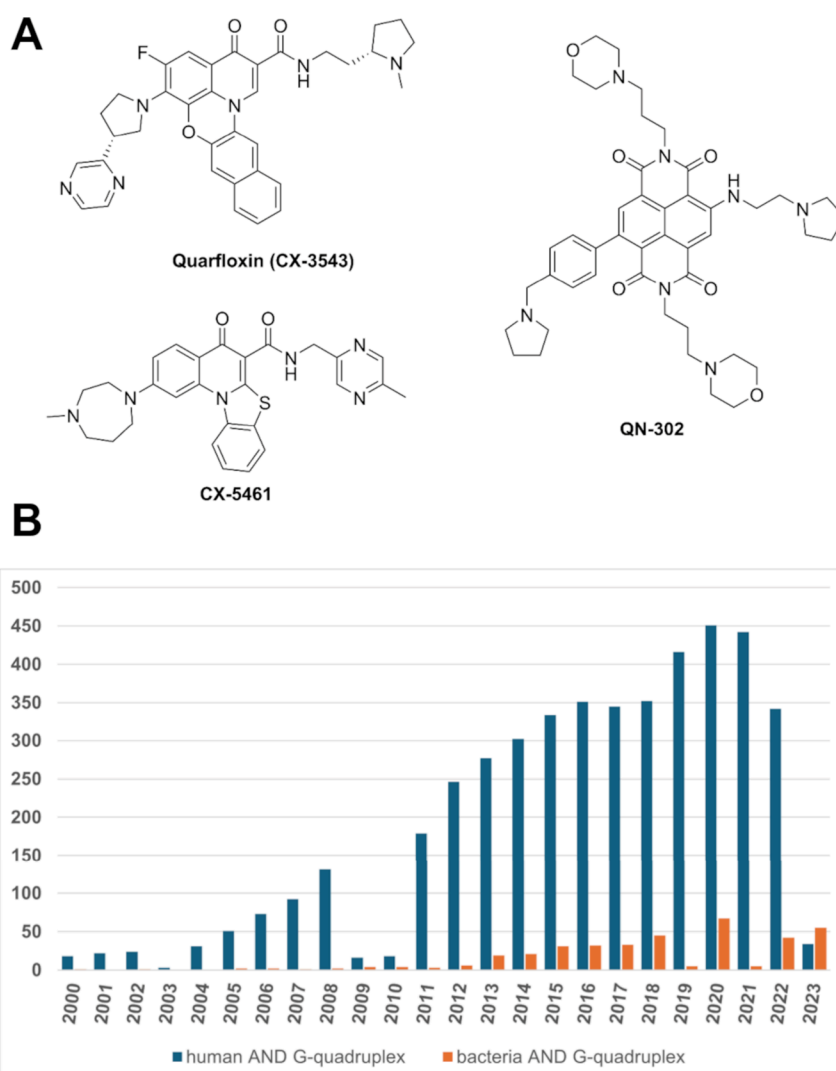


Figure 4. (A) Chemical structures of quarfloxin (CX-3543), CX-5461, and QN-302 as first-in-class stabilizers of human G4s investigated in clinical trials. (B) Trend of scientific publications retrieved from PubMed in the interval 2000–2023 using the keywords “human AND G-quadruplex” (blue bars) or “bacteria AND G-quadruplex” (orange bars). The search in PubMed was carried out at the end of January 20, 2024.

of genes involved in cycle control, cell division, and chromosome partitioning processes, in agreement with the observed bactericidal activity.¹²⁴

In the same work, NDI-10 exhibited a MIC of 16 μM against *S. aureus* (LMG8224 strain), showing a mainly bacteriostatic activity that has been associated with the stabilization of three G4 sequences (i.e., SA3, SA5, and SA7, Table 1) as depicted by the FRET melting assay. NDIs have emerged as valuable binders of human G4s as well as G4 sequences expressed in other microorganisms, including HIV-1, HSV-2, *T. brucei*, *L. major*, *P. falciparum*.¹²³

In 2022, the Galan group screened a small library of compounds against a panel of MDR *E. coli* strains and a reference susceptible strain (e.g., UTI808, IR60, and ATCC25922, respectively), identifying the azabenzene L20 (Figure 5) as the most promising hit with a MIC in the range 2–4 $\mu\text{g}/\text{mL}$.¹²⁷ Subsequently, target G4 sequences have been identified by proteomic analysis on cell lysates incubated with L20 as well as reference ligands including pyridostatin (PDS, Figure 5) through LC-MS/MS analysis, while the ligands' stabilizing efficacy has been evaluated by FRET melting on seven G4-putative sequences identified by LC-MS/MS in

pivotal genes (i.e., *dppA*, *thrA*, *yjbD*, *pdxA*, *clpB*, *glnD*, and *hemL*, Table 1). PDS is a 2-quinolonyl derivative that has been developed as a specific G4 binder in anticancer research, thanks to its stabilizing activity against telomeric G4s preventing telomeres elongation. PDS triggers the DNA-damage machinery leading to cell cycle arrest, senescence, and apoptosis.¹²⁸ Compared to PDS, L20 has shown only a moderate stabilizing effect, although it has a high selectivity for four G4 sequences corresponding to *glnD*, *pdxA*, *thrA*, and *yjbD* genes. This controversial result has led to the hypothesis that the antimicrobial activity of L20 might not be related to G4 stabilization, or its target sequences have not been identified by LC-MS/MS and further tested in the FRET melting assay. This latter option has been deemed with a higher priority, also considering that L20 has been found to affect the expression of G4-associated proteins and to modulate the expression of *E. coli* genes involved in the cellular translational machinery to a higher extent compared with PDS.¹²⁷ It is worth noting that well-known and widely used G4 stabilizers such as BRACO-19 and TMPyP4 (Figure 5) have shown no antimicrobial activity against *E. coli* and have not progressed further. TMPyP4 is 5,10,15,20-tetrakis(N-

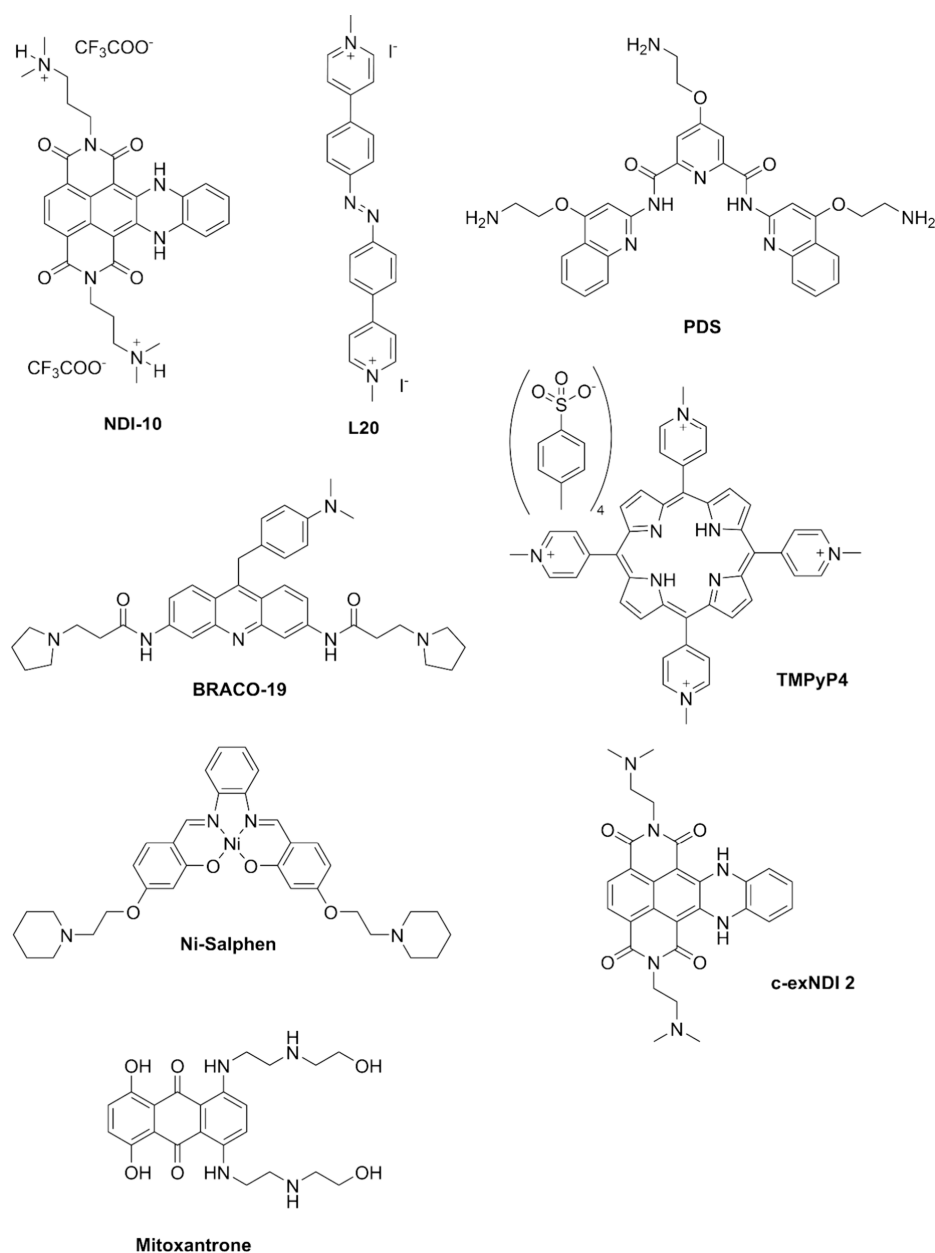


Figure 5. Chemical structure of G4s stabilizers tested against the bacterial G4s described in this work. Counterions were retrieved from the original publications or from commercial databases.

methyl-4-pyridyl)porphyrin, i.e., a cationic porphyrin that stacks on top of G-tetrads. **TMPyP4** is one of the most extensively investigated G4 binders, showing the induction of cancer cell death through downregulation of the expression of oncogenes such as *c-Myc*, *k-ras*, and *bcl2*.^{129–132} Thanks to its low cytotoxicity, **TMPyP4** is commonly employed to confirm putative G4 sequences in cell-based studies. From a chemical standpoint, **BRACO-19** is *N,N'*-(9-((4-(dimethylamino)phenyl)amino)acridine-3,6-diyl)bis(3-(pyrrolidin-1-yl)propanamide), a 3,6,9-trisubstituted acridine that has been extensively used as G4 stabilizer due to its high affinity for G4s compared to DNA duplexes.^{53,133–135} Indeed, the **BRACO-19** central core is mainly responsible for the π -stacking interactions at the top of terminal G-quartets, which are further reinforced by the protonated amine moieties in the side chains that engage in salt bridges with G4 grooves.

4.2. *Pseudomonas aeruginosa*. Another important example of G4-mediated gene regulation is represented by biofilm-producing bacteria. The biofilm plays a key role in the pathogenicity and infection persistence of bacteria such as *P. aeruginosa*, *N. gonorrhoeae*, *K. pneumoniae*, *P. denitrificans*, and *E. coli*. Among them, *P. aeruginosa* poses several interests and concerns for public health due to its opportunistic infections in immunocompromised patients, particularly in hospital environments. For these reasons, *P. aeruginosa* is included in the ESKAPE group. The biofilm is a complex aggregate in which the bacteria are enclosed, providing essential nutrients, enzymes, and cytosolic proteins for the biofilm community and facilitating the cell-to-cell communication, also known as quorum sensing.^{136–138} The biofilm is generally composed by a mixture of polysaccharides, extracellular DNA (eDNA), proteins, and lipids displaying a viscoelastic behavior.^{136,139} Moreover, the biofilm allows bacteria to escape both the host's

innate and adaptive immune responses, as well as to protect them from environmental stresses. Biofilm-producing bacteria are generally persistent for a long time and more resistant to antimicrobial treatments compared to their planktonic counterparts, often leading to chronic and/or persistent AMR infections. Therefore, developing antibiofilm agents is a current trend in drug development, although the lack of structural details and the variation of biofilm composition pose significant challenges.¹⁴⁰ The eDNA is enriched in G4-forming sequences compared to wild-type planktonic cells.¹⁴¹ Therefore, developing ligands that can stabilize G4s in the biofilm is expected to influence biofilm viscoelasticity and stability and the propagation and survival of biofilm-producing bacteria. Moreover, destabilization of the biofilm by G4 binders could potentially lead to decreased protection of bacteria, which might become more susceptible to antibiotics. Whether no ligands acting on biofilm-associated G4s have been developed or tested to date, the presence of G4s in the eDNA of *P. aeruginosa* biofilm has been confirmed by Seviour and colleagues using a combination of CD and NMR spectroscopy, as well as the G4-specific antibody clone 1H6, concluding that G4 modulation might be an effective strategy to control the biofilm of pathogenic bacteria.¹⁴²

Besides biofilm-associated G4s, in 2022 a bioinformatics study was conducted by Evans and collaborators to identify putative G4-forming sequences in the genome of *P. aeruginosa* using the QGRS Mapper web server.^{143,144} Among the ten putative sequences identified, CD spectroscopy and thermal difference UV-vis spectroscopy confirmed three sequences within pivotal genes *murE*, *ftsB*, and *mexC* (Table 1), which form stable G4s. By using ¹H NMR spectroscopy, the authors have been able to retrieve important structural details of *mexC* G4, whereas overlap in ¹H signals has impaired the solution of the structure for *murE* and *ftsB* G4s. With this information in hand, four well-known G4 binders (i.e., BRACO-19, PDS, TMPyP4, and Ni-salphen (Figure 5)) have been tested by a FRET melting assay for their interaction with the selected G4 sequences of *P. aeruginosa*. All tested molecules were able to stabilize G4s, with TMPyP4 showing the strongest efficacy among the small panel of tested compounds. Moreover, Ni-salphen has shown a moderate selectivity for *ftsB* and *mexC* G4s with respect to the *murE* G4, while PDS has been observed to stabilize the *ftsB* G4 with a two-step mechanism, suggesting that the ligand might shift among multiple binding sites or that it could bind to different topologies of the G4, even though further studies are needed to validate these hypotheses.¹⁴³

4.3. *Neisseria gonorrhoeae*. A notable example of G4 involvement in AMR mechanisms is represented by pilin antigen variation (AV) in *N. gonorrhoeae*,^{65,145,146} a Gram-negative bacterium responsible for the sexually transmitted disease gonorrhea in humans. The pilin genes are clustered in specific loci of the bacterial genome, and they codify for the pilins proteins that are fundamental for transformation (e.g., exchange of short DNA plasmids), twitching motility, and protection from the human immune system,^{147–149} the latter being achieved by exchanging portions of *pilE* with portions of the silent pilin sequences (*pilS*) through homologous recombination (HR). *PilE-pilS* AV is regulated by the formation of a G4 structure near the *pilE* promoter region.¹⁵⁰ Voter and colleagues have proposed a model based on the coordinated activities of Rec proteins family.¹⁵¹ Briefly, the helicase RecQ binds onto the *pilE* promoter region and

recruits RecJ, then RecQ unfolds the G4 structures while RecJ degrades the resulting single stranded DNA. Subsequently, the recombinase RecA recruits the DNA repair system, resulting in the restoration of the *pilE* gap using *pilS* as a template via HR. For this reason, *N. gonorrhoeae* escapes host immune system identification, preventing the adaptive response. This strategy is also employed by other bacteria of the same species, including *N. meningitidis*, which causes meningitis infections.¹⁵² Furthermore, similar strategies were adopted by other bacteria species, such as *B. burgdorferi*,¹⁵³ which causes the Lyme disease (borreliosis) transmitted by the bite of infected ticks in humans, and *T. pallidum*, which causes the sexually transmitted disease syphilis.¹⁵⁴ Besides, protozoans also take advantage of the AV strategy, such as *Trypanosomes*, which transmits the sleeping sickness in humans via blood-feeding invertebrates (*T. Brucei* and *T. Cruzi*), and *P. falciparum*, which causes the malaria disease transmitted by the bite of mosquito in humans.^{155,156}

Besides the relevance of G4 sequences involved in the pilin AV, no targeting ligands have been identified so far. In contrast, recent genome scanning for G4 putative sequences has been conducted on 83 genomes of *N. gonorrhoeae* using the in-house G4IPDB tool¹⁵⁷ as well as G4Hunter,⁷⁷ prioritizing five G4 motifs that are involved in important biological and molecular processes of *N. gonorrhoeae*.¹⁵⁸ Within pivotal genes in *N. gonorrhoeae*, the putative G4-forming sequences *norM*, *mtrC*, *modB*, *hldA*, and *gmhB* (Table 1) have been further characterized by multiple biophysical assays, including fluorescence and CD spectroscopy and 1D NMR, confirming the folding as G4s as well as providing hints on their individual topology. Subsequently, three reference G4 binders (BRACO-19, PDS, and TMPyP4, Figure 5) have been tested for their ability to bind and stabilize *N. gonorrhoeae* G4s. Among the tested ligands, BRACO-19 has emerged as the most effective binder and stabilizer of the five G4s tested in this work, as confirmed by fluorescence displacement, CD, isothermal titration calorimetry (ITC) suggesting an exothermic interaction, and 1D ¹H NMR assays.

BRACO-19 was originally tested against glioblastoma cells, uncapping telomeric structures and exposing the terminal part of the chromosome to DNA damage pathways to cause cell-cycle arrest, senescence, and short-term apoptosis.¹⁵⁹

In the study of BRACO-19's interaction with *N. gonorrhoeae* G4s, molecular modeling has further elucidated its binding mode preferences toward the five G4s identified as described above, showing G-tetrad stacking against *gmhB*, whereas loop and/or groove binding has been suggested for the other G4s. Finally, biological assays have been conducted with increasing concentrations of BRACO-19 with the aim to investigate its mechanism of action and its antimicrobial activity in vitro. Results have clearly showed that the G4 stabilizing activity of BRACO-19 stalled the Taq polymerase movement during DNA amplification and inhibited *N. gonorrhoeae* growth at low micromolar concentrations, in association with the modulation of the expression of key genes. Most notably, a dose-dependent decrease of *N. gonorrhoeae* biofilm height has been observed by treatment with BRACO-19, with the strongest efficacy having been recorded at 25 μ M ligand concentration, providing a decrease of 55% in biofilm production.¹⁵⁸

4.4. *Mycobacterium tuberculosis*. *M. tuberculosis* is a Gram-variable bacterium that induces a latent infection in lungs called tuberculosis, which is ranked in the top 10 causes of death worldwide.¹⁶⁰ *M. tuberculosis* infections are partic-

ularly challenging to treat due to two major factors: (i) the *M. tuberculosis* membrane composition ensures protection from innate immune system and drugs and (ii) several survival mechanisms operated by the bacterium prevent its eradication by the host and reduce the effectiveness of antibiotic therapy. Indeed, *M. tuberculosis* in the lung is phagocytosed by alveolar macrophages that are unable to digest the trehalose dimycolate (TDM) component of the bacterial wall, thus inhibiting the fusion of the phagosome with the lysosome.^{161,162} Additionally, *M. tuberculosis* produces isotuberculosinol, which prevents the maturation of the phagosome and neutralizes reactive nitrogen intermediates.^{163,164} *M. tuberculosis* also secretes 1-tuberculosinyladenosine that trigger inflammation in lysosomes, further promoting bacterial survival in granulomas.^{165–167} *M. tuberculosis* can survive in a latent and nonreplicative form in the host for decades until modifications of the environment, stress conditions, or a decrease in immune defenses can promote the reactivation of the infective stage of the bacterium.

In recent years, several putative G4-forming sequences have been identified within pivotal metabolic genes of the *M. tuberculosis* genome, including four sequences, i.e., glucose-6-phosphate dehydrogenase 1 (*zwf1*), ATP-dependent Clp protease (*clpX*), oxidation-sensing regulator transcription factor (*mosR*), and membrane NADH dehydrogenase (*ndhA*) (Table 1).¹⁶⁸ The putative G4-forming sequences in *M. tuberculosis* have been confirmed by CD spectroscopy, followed by their interactions with well-known G4s ligands, such as BRACO-19 and c-exNDI 2 (Figure 5). Notably, these molecules have been able to inhibit bacterial growth at micromolar doses.¹⁶⁸

Recently, by combining cell-based assays and biophysical investigations, G4s have been identified in *mosR* and *ndhA* genes involved in metabolic pathways. Notably, G4s in the *ndhA* gene overlap with the previous findings described above. The interaction of mitoxantrone (Figure 5) with the two G4 sequences has been monitored by biophysical tools, which showed the higher affinity of the molecule for the *ndhA* G4 compared to that for *mosR* G4, thus paving the way for further exploitation of the anthraquinone scaffold in the development of antibacterial agents targeting *M. tuberculosis* G4s.^{169,170}

Recently, three G4 structures have been prioritized by a bioinformatics scan of the genome of 160 *M. tuberculosis* strains.¹⁷¹ These G4s are highly conserved and are expressed in essential genes, i.e., *espK*, *espB*, and *cyp51* (Table 1), which are involved in *M. tuberculosis* virulence in the host and in the maintenance of membrane fluidity to enhance *M. tuberculosis* survival. G4 folding and topology were first confirmed by CD spectroscopy, which highlighted a predominant parallel topology as well as a strong stabilization in the presence of K⁺ ions. NMR spectroscopy has further confirmed the folding of these sequences as G4s. TMPyP4 (Figure 5) has been used as the reference ligand to assess the ability of G4s of *M. tuberculosis* to be stabilized by small molecules by CD melting and ITC assays, showing a stable interaction with an affinity constant in the low micromolar range against the three G4 species studied in the work. Finally, TMPyP4 has shown remarkable inhibition of *M. tuberculosis* growth in vitro, with an IC₅₀ of 6.25 μM and a significant modulation of the expression of *espK* and *espB* genes that corroborates the G4-mediated mechanism of action of TMPyP4 against *M. tuberculosis*.¹⁷¹

4.5. *Streptococcus pneumoniae*. The Gram-positive *S. pneumoniae* is one of the deadliest bacteria, causing pneumonia and meningitis in children and the elderly.¹⁷² *S. pneumoniae*

causes community-acquired pneumonia (CAP), which has a high fatality rate due to its PDR. Moreover, *S. pneumoniae* infections leaves deep scars in the surviving patients, generating neurological deficits, psychological impairment and hearing loss.¹⁷³ For these reasons, there is a considerable need to find alternative targets to contrast the *S. pneumoniae* AMR.

A bioinformatic and biophysical investigation was conducted in 2019 on the whole genome of 39 different strains of *S. pneumoniae*, leading to the identification of three highly conserved G4 sequences, i.e., *hsdS*, *recD*, and *pmrA* (Table 1), that control the restriction–modification systems, recombination, repair processes, and drug efflux systems, respectively.¹⁷⁴ Similar to previous investigations by the same authors, the G4 folding of these target sequences has been confirmed by CD and NMR spectroscopy and an electrophoretic mobility shift assay. TMPyP4 (Figure 5) has been used as a reference ligand to depict the ligand binding properties of target G4s by ITC and CD melting assays. Overall, TMPyP4 has shown energetically favorable and thermodynamically stable interactions with the G4 sequences, especially in comparison with its close analogue TMPyP2, which has shown weaker affinity and stabilization properties toward the G4 sequence.¹⁷⁴

4.6. *Vibrio cholerae*. *V. cholerae* is a Gram-negative bacterium that causes Cholera disease, infecting millions of people every year. In the last 200 years, *V. cholerae* caused seven major pandemics worldwide, and it is currently endemic in 47 countries.¹⁷⁵ Considering the worldwide spread, the high genomic plasticity, and the fast replication rates (~17 min), AMR strains of *V. cholerae* are raising serious concerns in public health systems.^{176–178} For these reasons, there is a need to identify a novel target to control *V. cholerae* infections. Recently, using bioinformatics tools, *in silico* simulations, and biophysical assays, several G4s were identified neighboring different ORFs such as the methyl-accepting chemotaxis proteins (MCPs), which is important for the chemotaxis of bacteria, the *rtxA* that codes for an exotoxin (Table 1), and GGDEF family proteins, which are important for the nucleotide cyclization process and osmolality sensor protein.^{179,180} The effective formation of G4 structures by these sequences has been confirmed by NMR, CD, and EMSA assays, whereas ligand binding properties have been monitored using the reference G4 binder TMPyP4 (Figure 5). Interestingly, molecular features of the interaction between TMPyP4 and target G4s have been depicted by molecular dynamics (MD) simulations, suggesting that the molecules mostly stack on the top of terminal G-tetrads.

Some G4s found in *V. cholerae* overlap with sequences found in other pathogenic bacteria such as *E. coli*, *K. pneumoniae*, *Y. pestis*, *S. flexneri*, *S. enterica*, *P. aeruginosa*, and *M. tuberculosis*, which paves the way to the potential development of broad-spectrum antibacterial agents endowed with a G4-related mechanism of action.

4.7. *Klebsiella pneumoniae*. *K. pneumoniae* is a Gram-negative member of the ESKAPE group causing lifelong diseases such as pneumonia, urinary tract infections, cystitis, endocarditis, sepsis, pyogenic liver abscesses, endogenous endophthalmitis necrotizing pneumonia, and bloodstream infections due to its AMR. Furthermore, *K. pneumoniae* is the major cause of nosocomial infections in hospital environments.^{181,182} Thus, there is a demand for alternative targets to overcome the *K. pneumoniae* AMR. To this aim, genome-wide screening and structural confirmation have been carried out on

Table 1. Summary of Main Features of Bacterial G4s Discussed in the Review

species	code	sequence (5'-3' direction)	T_m and K^+ concentration (CD)	T_m and K^+ concentration (FRET)
<i>E. coli</i>	EC-6	GGTGGGAGGGGTAAGGGG	60.0 ± 0.3 °C ($K^+ = 0.5$ mM)	49 ± 1 °C ($K^+ = 0.5$ mM)
<i>E. coli</i>	EC-9	GGGGCGGGTGGGTGG	63.7 ± 0.8 °C ($K^+ = 5$ mM)	52.6 ± 0.3 °C ($K^+ = 5$ mM)
<i>E. coli</i>	hemL	5'-FAM-GGTCCGGTCTATCAGGCGGGT-TAMRA-3'		59.0 °C ($K^+ = 100$ mM)
<i>E. coli</i>	dppA	5'-FAM-GGGCTGGACTGGCGATAACGGGG-TAMRA-3'		50.6 °C ($K^+ = 100$ mM)
<i>E. coli</i>	clpB	5'-FAM-GGCGGTTGGACGGGG-TAMRA-3'		63.6 °C ($K^+ = 100$ mM)
<i>E. coli</i>	yjbD	5'-FAM-GGGAAAAGGGTTAGGGTGAGGG-TAMRA-3'		53.1 °C ($K^+ = 100$ mM)
<i>E. coli</i>	thrA	5'-FAM-GGGCGATGGGGTAATGGTGCGGGGG-TAMRA-3'		56.1 °C ($K^+ = 100$ mM)
<i>E. coli</i>	pdxA	5'-FAM-GGGGAGTTGGGGGAATAAGGGCGGAGGG-TAMRA-3'		55.6 °C ($K^+ = 100$ mM)
<i>E. coli</i>	glnD	5'-FAM-GCGGTTGACCGGGCAGGGTGGG-TAMRA-3'		57.0 °C ($K^+ = 100$ mM)
<i>S. aureus</i>	SA-3	GGGGCTAATTGGGGCTGGTGG	61.0 ± 0.3 °C ($K^+ = 20$ mM)	54 ± 4 °C ($K^+ = 20$ mM)
<i>S. aureus</i>	SA-5	GGAAGGAGGGGTGACAGGG	64.2 ± 0.9 °C ($K^+ = 5$ mM)	55 ± 4 °C ($K^+ = 5$ mM)
<i>S. aureus</i>	SA-7	GGGTTTGGGGCGGGCGTTGG	59.4 ± 0.2 °C ($K^+ = 100$ mM)	51 ± 0.4 °C ($K^+ = 100$ mM)
<i>P. aeruginosa</i>	murE	GGTCGAGGCCAGGGCGGGG		57.2 ± 1.8 °C ^b ($K^+ = 100$ mM)
<i>P. aeruginosa</i>	ftsB	GGTACGGTGAAGGGGTGG		50.7 ± 0.2 °C ^b ($K^+ = 100$ mM)
<i>P. aeruginosa</i>	mexC	GGATCGGGCGTTGGCTATGG		45.6 ± 0.1 °C ^b ($K^+ = 100$ mM)
<i>N. gonorrhoeae</i>	gmhB-GQ	CTTTGGGTTGGGCGGGTTCGGGGGATG		
<i>N. gonorrhoeae</i>	hldA-GQ	TCTTGGGCGGGTGGGCTGGTAAATGGGTTCG		
<i>N. gonorrhoeae</i>	modB-GQ	TCAGGGCTTGGGTTGGGTTGGGTTG		
<i>N. gonorrhoeae</i>	mtrC-GQ	GCAGGGCGGGCAGCCTGCGGGTGGGAAAG		
<i>N. gonorrhoeae</i>	norM-GQ	AACGGGGCGGCAGGGGATTTGGTTCGGGCTGATTTGGGGAAC		
<i>M. tuberculosis</i>	zwf1	TGGGTTGTGGGCCAATGGGCTAGGGT	44.2 ± 1.4 °C ($K^+ = 50$ mM)	
			48.5 ± 0.5 °C ($K^+ = 100$ mM)	
			52.2 ± 1.9 °C ($K^+ = 150$ mM)	
<i>M. tuberculosis</i>	clpx	TGGGGGGCCGAGCAAGCGGGTAGCGTCGGGGCATAACGGGGT	52.0 ± 0.8 °C ($K^+ = 50$ mM)	
			59.2 ± 0.8 °C ($K^+ = 100$ mM)	
			74.2 ± 0.6 °C ($K^+ = 150$ mM)	
<i>M. tuberculosis</i>	mosR	TGGGCTAGCTCTAGGGGGCAGGGCTTTGACGGGT	49.4 ± 0.5 °C ($K^+ = 50$ mM)	
			50.8 ± 1.7 °C ($K^+ = 100$ mM)	
			51.7 ± 1.3 °C ($K^+ = 150$ mM)	
<i>M. tuberculosis</i>	ndhA	TGGGCCCTGTGGGCCCTTGTGGCCCTGTGGGT	$45.4 \pm 1.6/71.2 \pm 2.1$ °C ^a ($K^+ = 50$ mM)	
			$38.1 \pm 0.4/74.4 \pm 1.3$ °C ^a ($K^+ = 100$ mM)	
			$52.6 \pm 3.1/80.2 \pm 1.3$ °C ^a ($K^+ = 150$ mM)	
<i>M. tuberculosis</i>	espK	GGGGTCCCGGGGTGATCGGGTTCGGGGG	73.2 °C ($K^+ = 50$ mM)	
<i>M. tuberculosis</i>	espB	GGGCGGGGTGGCATGGGAATGCCGATGGGTGCCCGGCATCAGGG	81.22 °C ($K^+ = 50$ mM)	
<i>M. tuberculosis</i>	cyp51	GGGATCGGGGAAGTCTTCGGGGATCCGGTTGGAGATCGCCGGGG	57.86 °C ($K^+ = 50$ mM)	

Table 1. continued

species	code	sequence (5'-3' direction)	T_m and K^+ concentration (CD)	T_m and K^+ concentration (FRET)
<i>S. pneumoniae</i>	recD	GGGCAACTTGGCTGGGGTCTAGTTCACGGGACGGG	50.96 °C (K^+ = 50 mM) 52.81 °C (K^+ = 200 mM)	
<i>S. pneumoniae</i>	hsdS	GGGCTAGTGGGGGAGGG	52.38 °C (K^+ = 50 mM) 56.75 °C (K^+ = 200 mM)	
<i>S. pneumoniae</i>	pmrA	GGGCTAATAGGGAGAGCAGGGACGGGG	51.34 °C (K^+ = 50 mM) 55.68 °C (K^+ = 200 mM)	
<i>V. cholerae</i>	RTX	the whole sequence described in the original publication is deposited in the GenBank database, accession number AF119150 (https://www.ncbi.nlm.nih.gov/nucleotide/AF119150)		
<i>K. pneumoniae</i>	KP-PGQ-3	GGGGAGAGGGGAAGGGTGAGGG	53.75 °C (K^+ = 50 mM) 57.94 °C (K^+ = 200 mM)	
<i>K. pneumoniae</i>	KP-PGQ-5	GGGAGAGGGCCGGGGTGAGGG	58.61 °C (K^+ = 50 mM) 63.58 °C (K^+ = 200 mM)	
<i>H. pylori</i>	nixA	GGGGGGTAGTGGGGACTTTAGTTTCTGGG	60.78 °C (K^+ = 50 mM)	
<i>H. pylori</i>	niuD	GGGATTCTAGCGGGGCGATGCTAGCGGTGG	52.75 °C (K^+ = 50 mM)	
<i>H. pylori</i>	niuB2	GGAATAGGGTTGTAGGCGTTTCGG	54.95 °C (K^+ = 50 mM)	
<i>H. pylori</i>	niuB1	GGGATAGGGTCGTGGGAATTCGG	57.16 °C (K^+ = 50 mM)	

^aWhen multiple T_m values are reported, they correspond to different G4 species described in the original publication. ^bIn the original publication, this value is reported as a $T_{1/2}$.

G4 forming sequences in *K. pneumoniae*, highlighting several highly conserved G4 putative sequences that control pivotal genes involved in metabolism, such as D-erythrose 4-phosphate dehydrogenase (*epd*), alcohol dehydrogenase (lactaldehyde reductase), L-ribulose-5-phosphate 4-epimerase (*araD*), ABC transporter, and 2,4-dienoyl-CoA reductase. While EMSA, NMR, and CD spectroscopy have confirmed the stable formation of G4 structures, the formation of stable intramolecular G4s with a predominant mixed hybrid topology in the presence of K^+ ions has been recorded, with only two sequences (i.e., KP-PGQ-3 and KP-PGQ-5 (Table 1)) showing a predominant parallel topology.¹⁸³ Furthermore, the interaction of these G4s of *K. pneumoniae* with BRACO-19 (Figure 5) has been investigated by CD melting and ITC, showing a mostly exothermic interaction that becomes endothermic with time dependency. The association constant K_a has been found at the highest value for the interaction with KP-PGQ-3 ($K_a = 5.92 \times 10^{11} \text{ M}^{-1}$), highlighting a binding preference of BRACO-19 for parallel G4s. BRACO-19 has also been tested in a cellular model system using the MTT assay, resulting in *K. pneumoniae* ATCC700603 growth inhibition with an IC_{50} of 10.77 μM , an effect that has been associated with decreased expression of genes harboring the target and highly conserved G4 sequences. These results provided by qPCR corroborate the potential interaction of BRACO-19 with *K. pneumoniae* G4s in vivo.¹⁸³

4.8. Helicobacter pylori. *H. pylori* is a Gram-negative bacterium that populates the gastric mucus located in the human stomach, causing chronic gastritis, peptic ulcer disease, MALT lymphoma, and gastric adenocarcinoma. Noteworthy, it is estimated that 50% of the world's human population is infected by *H. pylori*.¹⁸⁴ Until the 80s, the stomach environment has been considered unfavorable for the growth and survival of bacteria, which has favored the spread of *H. pylori* infections as well as the emergence of AMR strains.¹⁸⁵ Since *H. pylori* causes chronic infections that led to stomach cancer, there is an interest in developing effective antibiotics to

overcome its growth as well as AMR. For these reasons, the *H. pylori* genome was investigated, with the aim of finding G4 forming sequences. Several putative G4s were identified in essential genes involved in metabolic pathways, nucleotide binding, metal binding, etc. The *nixA*, *niuB1*, *niuB2*, and *niuD* (Table 1) are Ni^{2+} transport-associated genes for which a G4 structure was confirmed by multiple spectroscopic techniques.¹⁸⁶ The Ni^{2+} homeostasis is pivotal for urease and Ni/Fe dehydrogenase activation which are required for the survival and growth of *H. pylori* in the human gastric environment.¹⁸⁷ In analogy with other studies carried out by the research team, TMPyP4 (Figure 5) was used as a reference G4 binder to monitor the ligand-binding properties of target *H. pylori* G4 sequences, as well as to monitor the expression of Ni^{2+} transport-associated genes.¹⁸⁶

5. DRUG-LIKENESS ISSUES OF CURRENT G4 BINDERS

Although some of the results described above might be conceived as preliminary and need additional investigations and confirmations, they corroborate the potential druggability of bacterial G4 sequences by small molecules. The most effective mechanism of action reported to date is G4 stabilization by chemical binders able to interact with G-tetrads by means of π -stacking or hydrophobic interactions, which can be further reinforced by electrostatic and H-bond interactions. Indeed, looking at the chemical structures of Figure 5, G4 stabilizers share some common features such as an extended aromatic core, which is assumed to stack on the top of G-tetrads, and a number of positively charged or chargeable basic groups that surround the aromatic core and are expected to interact with the phosphate backbone. Despite their efficacy in G4 stabilization and, in some examples, their antibacterial properties, these molecules are unfortunately endowed with a poor drug-likeness, mostly because their flatness, abundance of positively charged groups that impair passive cellular uptake, and violations of Lipinski's rule of five (e.g., high molecular weight, which significantly decrease the

bioavailability).¹⁸⁸ Moreover, most of the ligands described herein have been reported to also stabilize G4s from different species, including *Homo sapiens*, and some viruses such as HIV-1 and HCV, which points to the lack of specificity for a target G4 and to the potential cytotoxicity of these molecules due to off-target interactions.^{134,189–191} From a structural standpoint, this drawback is related to the interaction with G-tetrads, i.e., the most conserved structural element of G4s, which renders these molecules good tools for biochemical/biophysical studies but weak candidates for pharmacological aims. In contrast, given the sequence and structural features of G4s described above, small molecules designed to interact with G4 grooves or loops are expected to exert a very high specificity for a target G4 because these are the most variable portions of G4s.¹⁹² To date, only a few examples of G4 groove binders have been reported,^{193–198} suggesting that these compounds are endowed with a significantly higher drug-likeness than G-tetrad binders and making them potential lead candidates for drug development. The design of G4 groove binders is currently challenging due to the lack of exploitable structural details. However, biophysical studies coupled with computational investigations might overcome these issues and can strongly promote a new trend in the development of G4 binders of pharmaceutical relevance.

6. CONCLUSIONS

Bacterial G4s are attractive targets for antimicrobial drug discovery, given that specific and drug-like G4 binders are expected to provide antibacterial activity as well as synergize with existing drugs. While the effective translational potential of bacterial G4s modulators is currently limited by the use of undruggable biochemical tools (such as compounds in Figure 5), it is expected that this relatively new field will remarkably grow in the near future, leading to the disclosure of drug-like modulators of bacterial G4s that can eventually be developed up to preclinical or clinical candidates. However, the current knowledge on the structure, function, and druggability of bacterial G4s is limited, especially compared to human G4s, which highlights the need for concerted and multidisciplinary efforts. In particular, structural features of bacterial G4s are mostly unavailable, which raises the opportunity for bioinformaticians and computational structural biologists to develop predictive tools able to quickly model at least a rough G4 structure based on sequence features, which can be further exploited in structure-based drug design approaches.

7. SEARCH CRITERIA FOR STRUCTURAL DATA

Structures of G4s shown in Figure 2 have been searched in the Protein Data Bank (PDB) at <https://www.rcsb.org/>. In the advanced search tab, the following options have been used:

- “quadruplex” as a search term in the Full text box
- “bacteria” as an additional search term in a second Full text box
- “Entry Polymer Type is Nucleic acid (only)” as a filter in the Structure Attributes box
- “Structure Title is NOT (has any of words) human”
- “Source Organism Taxonomy Name is NOT viruses” in the Structure Attributes box
- “Scientific Name of the Source Organism is NOT synthetic construct” in the Structure Attributes box

A visual inspection and analysis of results obtained by the search criteria listed above have resulted in 30 structures,

among which only 2 have been effectively attributed to bacterial G4s. The remaining 28 structures correspond to structural studies of custom or modified sequences that adopt G4 folding.

Statistical data shown in Figure 4 have been extracted from PubMed at <https://pubmed.ncbi.nlm.nih.gov/> by applying the following search criteria:

- “human AND G-quadruplex”
- “bacteria AND G-quadruplex”

Results were then exported in csv format and filtered in the interval from 2000 to 2023 before being used to generate the corresponding graphs.

AUTHOR INFORMATION

Corresponding Author

Mattia Mori – Department of Biotechnology, Chemistry and Pharmacy, University of Siena, 53100 Siena, Italy;
orcid.org/0000-0003-2398-1254; Phone: +39 0577 232360; Email: mattia.mori@unisi.it

Authors

Stefano Ciaco – Department of Biotechnology, Chemistry and Pharmacy, University of Siena, 53100 Siena, Italy;
orcid.org/0000-0003-0624-7496
Rossella Aronne – Department of Biotechnology, Chemistry and Pharmacy, University of Siena, 53100 Siena, Italy;
orcid.org/0009-0008-3513-8188
Martina Fiabane – Department of Biotechnology, Chemistry and Pharmacy, University of Siena, 53100 Siena, Italy;
orcid.org/0009-0009-2438-9018

Complete contact information is available at:
<https://pubs.acs.org/10.1021/acsomega.4c01731>

Notes

The authors declare no competing financial interest.

ACKNOWLEDGMENTS

This study has received funding from the EU's Horizon Europe research and innovation program under HORIZON-MSCA-2022-PF-01, Grant 101106871 (S.C.); from the EU's Next Generation EU-MUR PNRR Extended Partnership initiative on Emerging Infectious Diseases (project no. PE00000007, INF-ACT) (M.M., M.F.), and from the European Union's Next Generation EU-Italian Ministry of University and Research (MUR), project PRIN-PNRR P2022BWS27 (G4MICRONAT) (M.M., R.A.).

REFERENCES

- (1) Venkatesan, P. WHO 2020 report on the antibacterial production and development pipeline. *Lancet Microbe* **2021**, *2* (6), No. e239.
- (2) WHO publishes list of bacteria for which new antibiotics are urgently needed. *World Health Organization*, 2017. <https://www.who.int/news/item/27-02-2017-who-publishes-list-of-bacteria-for-which-new-antibiotics-are-urgently-needed> (accessed 2024-02-15).
- (3) De Oliveira, D. M. P.; Forde, B. M.; Kidd, T. J.; Harris, P. N. A.; Schembri, M. A.; Beatson, S. A.; Paterson, D. L.; Walker, M. J. Antimicrobial Resistance in ESKAPE Pathogens. *Clin Microbiol Rev.* **2020**, DOI: 10.1128/CMR.00181-19.
- (4) Review on Antimicrobial Resistance. *Antimicrobial Resistance: Tackling a crisis for the health and wealth of nations*; Wellcome Trust: London, UK, 2014. <https://amr-review.org/sites/default/files/A%20R%20Review%20Paper%20-%20>

%20Tackling%20a%20crisis%20for%20the%20health%20and%20wealth%20of%20nations_1.pdf (accessed 2024-2-15).

(5) Landovitz, R. J.; Scott, H.; Deeks, S. G. Prevention, treatment and cure of HIV infection. *Nat. Rev. Microbiol* **2023**, *21* (10), 657–670.

(6) Bhattacharjee, C.; Singh, M.; Das, D.; Chaudhuri, S.; Mukhopadhyay, A. Current therapeutics against HCV. *Virusdisease* **2021**, *32* (2), 228–243.

(7) GBD 2019 Antimicrobial Resistance Collaborators. Global mortality associated with 33 bacterial pathogens in 2019: a systematic analysis for the Global Burden of Disease Study 2019. *Lancet* **2022**, *400* (10369), 2221–2248.

(8) Plackett, B. Why big pharma has abandoned antibiotics. *Nature* **2020**, *586*, S50–S52, DOI: 10.1038/d41586-020-02884-3.

(9) Hutchings, M. I.; Truman, A. W.; Wilkinson, B. Antibiotics: past, present and future. *Curr. Opin Microbiol* **2019**, *51*, 72–80.

(10) The world is running out of antibiotics, WHO report confirms. *World Health Organization*, 2017. <https://www.who.int/news/item/20-09-2017-the-world-is-running-out-of-antibiotics-who-report-confirms> (accessed 2024-02-15).

(11) WHO. 2020 Antibacterial agents in clinical and preclinical development: An overview and analysis; World Health Organization: Geneva, Switzerland, 2021.

(12) Cusinato, J.; Cau, Y.; Calvani, A. M.; Mori, M. Repurposing drugs for the management of COVID-19. *Expert Opin Ther Pat* **2021**, *31* (4), 295–307.

(13) Harrison, C. Coronavirus puts drug repurposing on the fast track. *Nat. Biotechnol.* **2020**, *38* (4), 379–381.

(14) Williams, B. A.; Jones, C. H.; Welch, V.; True, J. M. Outlook of pandemic preparedness in a post-COVID-19 world. *Npj Vaccines* **2023**, *8*, 178.

(15) Dolgin, E. How COVID unlocked the power of RNA vaccines. *Nature* **2021**, *589* (7841), 189–191.

(16) Dolgin, E. The tangled history of mRNA vaccines. *Nature* **2021**, *597* (7876), 318–324.

(17) Barrantes, F. J. The Contribution of Biophysics and Structural Biology to Current Advances in COVID-19. *Annu. Rev. Biophys* **2021**, *50*, 493–523.

(18) Barcena, M.; Barnes, C. O.; Beck, M.; Bjorkman, P. J.; Canard, B.; Gao, G. F.; Gao, Y.; Hilgenfeld, R.; Hummer, G.; Patwardhan, A.; Santoni, G.; Saphire, E. O.; Schaffitzel, C.; Schendel, S. L.; Smith, J. L.; Thorn, A.; Veessler, D.; Zhang, P.; Zhou, Q. Structural biology in the fight against COVID-19. *Nat. Struct. Mol. Biol.* **2021**, *28* (1), 2–7.

(19) Yang, H.; Rao, Z. Structural biology of SARS-CoV-2 and implications for therapeutic development. *Nat. Rev. Microbiol* **2021**, *19* (11), 685–700.

(20) Hicks, L.; Evans, C.; Gerber, J.; Patel, P. What Clinicians, Pharmacists, and Public Health Partners Need to Know about Antibiotic Prescribing and COVID-19. *CDC Emergency Preparedness and Response*, 2021. https://emergency-origin.cdc.gov/coca/calls/2021/callinfo_111821.asp?cid=EPRhomepage (accessed 2024-02-15).

(21) CDC COVID-19: U.S. impact on antimicrobial resistance, special report 2022; U.S. Department of Health and Human Services: Washington, D.C., 2022.

(22) Berman, H. M.; Westbrook, J.; Feng, Z.; Gilliland, G.; Bhat, T. N.; Weissig, H.; Shindyalov, I. N.; Bourne, P. E. The Protein Data Bank. *Nucleic Acids Res.* **2000**, *28* (1), 235–42.

(23) Coimbatore Narayanan, B.; Westbrook, J.; Ghosh, S.; Petrov, A. I.; Sweeney, B.; Zirbel, C. L.; Leontis, N. B.; Berman, H. M. The Nucleic Acid Database: new features and capabilities. *Nucleic Acids Res.* **2014**, *42*, D114.

(24) Picarazzi, F.; Vicenti, I.; Saladini, F.; Zazzi, M.; Mori, M. Targeting the RdRp of Emerging RNA Viruses: The Structure-Based Drug Design Challenge. *Molecules* **2020**, *25* (23), 5695.

(25) Oelschlaeger, P. beta-Lactamases: Sequence, Structure, Function, and Inhibition. *Biomolecules* **2021**, *11* (7), 986.

(26) Picarazzi, F.; Mori, M. DNA and RNA polymerases. *Metalloenzymes* **2024**, 9–22.

(27) Engelman, A.; Cherepanov, P. The structural biology of HIV-1: mechanistic and therapeutic insights. *Nat. Rev. Microbiol* **2012**, *10* (4), 279–90.

(28) Dutescu, I. A.; Hillier, S. A. Encouraging the Development of New Antibiotics: Are Financial Incentives the Right Way Forward? A Systematic Review and Case Study. *Infect Drug Resist* **2021**, *14*, 415–434.

(29) Global Leaders Group on Antimicrobial Resistance. *Financing to Address Antimicrobial Resistance*; World Health Organization: Geneva, Switzerland, 2021. https://cdn.who.int/media/docs/default-source/antimicrobial-resistance/amr-gcp-tjs/financing-to-address-amr.pdf?sfvrsn=c982548e_10 (accessed 2024-02-15).

(30) Seguin-Devaux, C.; Mestrovic, T.; Arts, J. J.; Karaman, D. S.; Nativi, C.; Reichmann, D.; Sahariah, P.; Smani, Y.; Rijo, P.; Mori, M. Solving the antibacterial resistance in Europe: the multipronged approach of the COST Action CA21145 EURESTOP. *Drug Resistance Updates* **2024**, *74*, No. 101069.

(31) Ovchinnikov, S.; Kinch, L.; Park, H.; Liao, Y.; Pei, J.; Kim, D. E.; Kamisetty, H.; Grishin, N. V.; Baker, D. Large-scale determination of previously unsolved protein structures using evolutionary information. *eLife* **2015**, *4*, No. e09248.

(32) Ovchinnikov, S.; Park, H.; Varghese, N.; Huang, P. S.; Pavlopoulos, G. A.; Kim, D. E.; Kamisetty, H.; Kyrpides, N. C.; Baker, D. Protein structure determination using metagenome sequence data. *Science* **2017**, *355* (6322), 294–298.

(33) Soding, J. Big-data approaches to protein structure prediction. *Science* **2017**, *355* (6322), 248–249.

(34) Jumper, J.; Evans, R.; Pritzel, A.; Green, T.; Figurnov, M.; Ronneberger, O.; Tunyasuvunakool, K.; Bates, R.; Zidek, A.; Potapenko, A.; Bridgland, A.; Meyer, C.; Kohl, S. A. A.; Ballard, A. J.; Cowie, A.; Romera-Paredes, B.; Nikolov, S.; Jain, R.; Adler, J.; Back, T.; Petersen, S.; Reiman, D.; Clancy, E.; Zielinski, M.; Steinegger, M.; Pacholska, M.; Berghammer, T.; Bodenstein, S.; Silver, D.; Vinyals, O.; Senior, A. W.; Kavukcuoglu, K.; Kohli, P.; Hassabis, D. Highly accurate protein structure prediction with AlphaFold. *Nature* **2021**, *596* (7873), 583–589.

(35) van Breugel, M.; Rosa, E. S. I.; Andreeva, A. Structural validation and assessment of AlphaFold2 predictions for centrosomal and centriolar proteins and their complexes. *Commun. Biol.* **2022**, *5*, 312.

(36) Rothberg, J. M.; Leamon, J. H. The development and impact of 454 sequencing. *Nat. Biotechnol.* **2008**, *26* (10), 1117–24.

(37) Weinstock, G.; Goldberg, B.; Ledebor, N.; Rubin, E.; Sichtig, H.; Geyer, C. *Applications of Clinical Microbial Next-Generation Sequencing*; American Society for Microbiology: Washington, D.C., 2016.

(38) Tassios, P. T.; Moran-Gilad, J. Bacterial next generation sequencing (NGS) made easy. *Clin Microbiol Infect* **2018**, *24* (4), 332–334.

(39) Sheng, J.; Gan, J.; Huang, Z. Structure-based DNA-targeting strategies with small molecule ligands for drug discovery. *Med. Res. Rev.* **2013**, *33* (5), 1119–73.

(40) Childs-Disney, J. L.; Yang, X.; Gibaut, Q. M. R.; Tong, Y.; Batey, R. T.; Disney, M. D. Targeting RNA structures with small molecules. *Nat. Rev. Drug Discov* **2022**, *21* (10), 736–762.

(41) Harrell, W. A., Jr. *Quadruplex Nucleic Acids*; Neidle, S., Balasubramanian, S., Eds.; Royal Society of Chemistry: London, UK, 2006.

(42) Todd, A. K.; Johnston, M.; Neidle, S. Highly prevalent putative quadruplex sequence motifs in human DNA. *Nucleic Acids Res.* **2005**, *33* (9), 2901–7.

(43) Balasubramanian, S.; Neidle, S. G-quadruplex nucleic acids as therapeutic targets. *Curr. Opin Chem. Biol.* **2009**, *13* (3), 345–53.

(44) Balasubramanian, S.; Hurley, L. H.; Neidle, S. Targeting G-quadruplexes in gene promoters: a novel anticancer strategy? *Nat. Rev. Drug Discov* **2011**, *10* (4), 261–75.

(45) Li, Y.; Chi, J.; Xu, P.; Dong, X.; Le, A.-T.; Shi, K.; Liu, Y.; Xiao, J. Supramolecular G-quadruplex hydrogels: Bridging fabrication to biomedical application. *J. Mater. Sci. Technol.* **2023**, *155*, 238–252.

- (46) Lopes-Nunes, J.; Oliveira, P.; Cruz, C. G-Quadruplex-Based Drug Delivery Systems for Cancer Therapy. *Pharmaceuticals* **2021**, *14* (7), 671.
- (47) Saranathan, N.; Vivekanandan, P. G-Quadruplexes: More Than Just a Kink in Microbial Genomes. *Trends Microbiol* **2019**, *27* (2), 148–163.
- (48) Lyu, B.; Song, Q. S. The intricate relationship of G-Quadruplexes and bacterial pathogenicity islands. *eLife* **2024**, *12*, RP91985.
- (49) Spiegel, J.; Adhikari, S.; Balasubramanian, S. The Structure and Function of DNA G-Quadruplexes. *Trends Chem.* **2020**, *2* (2), 123–136.
- (50) Viglasky, V.; Bauer, L.; Tluczkova, K. Structural features of intra- and intermolecular G-quadruplexes derived from telomeric repeats. *Biochemistry* **2010**, *49* (10), 2110–20.
- (51) Banco, M. T.; Ferre-D'Amare, A. R. The emerging structural complexity of G-quadruplex RNAs. *RNA* **2021**, *27* (4), 390–402.
- (52) Neidle, S. Quadruplex Nucleic Acids as Novel Therapeutic Targets. *J. Med. Chem.* **2016**, *59* (13), 5987–6011.
- (53) Ruggiero, E.; Richter, S. N. G-quadruplexes and G-quadruplex ligands: targets and tools in antiviral therapy. *Nucleic Acids Res.* **2018**, *46* (7), 3270–3283.
- (54) Yang, D. G-Quadruplex DNA and RNA. *Methods Mol. Biol.* **2019**, *2035*, 1–24.
- (55) Largy, E.; Mergny, J. L.; Gabelica, V. Role of Alkali Metal Ions in G-Quadruplex Nucleic Acid Structure and Stability. *Met. Ions Life Sci.* **2016**, *16*, 203–258.
- (56) Harrell, W. A., Jr., Fundamentals of Quadruplex Structures. In *Quadruplex Nucleic Acids*, Neidle, S., Balasubramanian, S., Eds. Royal Society of Chemistry: London, UK, 2006; pp 1–30.
- (57) Wong, A.; Wu, G. Selective binding of monovalent cations to the stacking G-quartet structure formed by guanosine 5'-monophosphate: a solid-state NMR study. *J. Am. Chem. Soc.* **2003**, *125* (45), 13895–905.
- (58) Howard, F. B.; Frazier, J.; Miles, H. T. Stable and metastable forms of poly(G). *Biopolymers* **1977**, *16* (4), 791–809.
- (59) Burge, S.; Parkinson, G. N.; Hazel, P.; Todd, A. K.; Neidle, S. Quadruplex DNA: sequence, topology and structure. *Nucleic Acids Res.* **2006**, *34* (19), 5402–15.
- (60) Ma, Y.; Iida, K.; Nagasawa, K. Topologies of G-quadruplex: Biological functions and regulation by ligands. *Biochem. Biophys. Res. Commun.* **2020**, *531* (1), 3–17.
- (61) Hsu, S. T.; Varnai, P.; Bugaut, A.; Reszka, A. P.; Neidle, S.; Balasubramanian, S. A G-rich sequence within the c-kit oncogene promoter forms a parallel G-quadruplex having asymmetric G-tetrad dynamics. *J. Am. Chem. Soc.* **2009**, *131* (37), 13399–409.
- (62) Wang, Z. F.; Li, M. H.; Hsu, S. T.; Chang, T. C. Structural basis of sodium-potassium exchange of a human telomeric DNA quadruplex without topological conversion. *Nucleic Acids Res.* **2014**, *42* (7), 4723–33.
- (63) Piazza, A.; Adrian, M.; Samazan, F.; Heddi, B.; Hamon, F.; Serero, A.; Lopes, J.; Teulade-Fichou, M. P.; Phan, A. T.; Nicolas, A. Short loop length and high thermal stability determine genomic instability induced by G-quadruplex-forming minisatellites. *EMBO J.* **2015**, *34* (12), 1718–1734.
- (64) Winnerdy, F. R.; Phan, A. T. Quadruplex structure and diversity. *Annu. Rev. Med. Chem.* **2020**, *54*, 45–73.
- (65) Kuryavyi, V.; Cahoon, L. A.; Seifert, H. S.; Patel, D. J. RecA-binding pilE G4 sequence essential for pilin antigenic variation forms monomeric and 5' end-stacked dimeric parallel G-quadruplexes. *Structure* **2012**, *20* (12), 2090–102.
- (66) Wang, Y.; Patel, D. J. Solution structure of the Tetrahymena telomeric repeat d(T2G4)4 G-tetraplex. *Structure* **1994**, *2* (12), 1141–56.
- (67) Kwok, C. K.; Sherlock, M. E.; Bevilacqua, P. C. Effect of loop sequence and loop length on the intrinsic fluorescence of G-quadruplexes. *Biochemistry* **2013**, *52* (18), 3019–21.
- (68) Gustavsson, T.; Markovitsi, D. Fundamentals of the Intrinsic DNA Fluorescence. *Acc. Chem. Res.* **2021**, *54* (5), 1226–1235.
- (69) Hayden, K. L.; Graves, D. E. Addition of bases to the 5'-end of human telomeric DNA: influences on thermal stability and energetics of unfolding. *Molecules* **2014**, *19* (2), 2286–98.
- (70) Seo, Y. J.; Lee, I. J.; Kim, B. H. Detection of structure-switching in G-quadruplexes using end-stacking ability. *Bioorg. Med. Chem. Lett.* **2008**, *18* (14), 3910–3.
- (71) del Villar-Guerra, R.; Trent, J. O.; Chaires, J. B. G-Quadruplex Secondary Structure Obtained from Circular Dichroism Spectroscopy. *Angew. Chem. Int. Edit.* **2018**, *57* (24), 7171–7175.
- (72) D'Anna, L.; Miclot, T.; Bignon, E.; Perricone, U.; Barone, G.; Monari, A.; Terenzi, A. Resolving a guanine-quadruplex structure in the SARS-CoV-2 genome through circular dichroism and multiscale molecular modeling. *Chem. Sci.* **2023**, *14* (41), 11332–11339.
- (73) Miclot, T.; Hognon, C.; Bignon, E.; Terenzi, A.; Marazzi, M.; Barone, G.; Monari, A. Structure and Dynamics of RNA Guanine Quadruplexes in SARS-CoV-2 Genome. Original Strategies against Emerging Viruses. *J. Phys. Chem. Lett.* **2021**, *12* (42), 10277–10283.
- (74) Bugaut, A.; Balasubramanian, S. A sequence-independent study of the influence of short loop lengths on the stability and topology of intramolecular DNA G-quadruplexes. *Biochemistry* **2008**, *47* (2), 689–97.
- (75) Dey, U.; Sarkar, S.; Teronpi, V.; Yella, V. R.; Kumar, A. G-quadruplex motifs are functionally conserved in cis-regulatory regions of pathogenic bacteria: An in-silico evaluation. *Biochimie* **2021**, *184*, 40–51.
- (76) Puig Lombardi, E.; Londono-Vallejo, A. A guide to computational methods for G-quadruplex prediction. *Nucleic Acids Res.* **2020**, *48* (1), 1–15.
- (77) Brazda, V.; Kolomaznik, J.; Lysek, J.; Bartas, M.; Fojta, M.; Stastny, J.; Mergny, J. L. G4Hunter web application: a web server for G-quadruplex prediction. *Bioinformatics* **2019**, *35* (18), 3493–3495.
- (78) Luo, Y.; Granzhan, A.; Marquavielle, J.; Cucchiari, A.; Lacroix, L.; Amrane, S.; Verga, D.; Mergny, J. L. Guidelines for G-quadruplexes: I. In vitro characterization. *Biochimie* **2023**, *214*, 5–23.
- (79) Kwok, C. K.; Merrick, C. J. G-Quadruplexes: Prediction, Characterization, and Biological Application. *Trends Biotechnol* **2017**, *35* (10), 997–1013.
- (80) Santos, T.; Salgado, G. F.; Cabrita, E. J.; Cruz, C. G-Quadruplexes and Their Ligands: Biophysical Methods to Unravel G-Quadruplex/Ligand Interactions. *Pharmaceuticals* **2021**, *14* (8), 769.
- (81) Tinoco, I., Jr. Hypochromism in polynucleotides. *J. Am. Chem. Soc.* **1960**, *82*, 4785–4790.
- (82) Rhodes, W. HYPOCHROMISM AND OTHER SPECTRAL PROPERTIES OF HELICAL POLYNUCLEOTIDES. *J. Am. Chem. Soc.* **1961**, *83*, 3609–3617.
- (83) Dao, N. T.; Haselsberger, R.; Michel-Beyerle, M. E.; Phan, A. T. Following G-quadruplex formation by its intrinsic fluorescence. *FEBS Lett.* **2011**, *585* (24), 3969–77.
- (84) Tevonyan, L. L.; Beniaminov, A. D.; Kaluzhny, D. N. Quenching of G4-DNA intrinsic fluorescence by ligands. *Eur. Biophys J.* **2024**, *53* (1–2), 47–56.
- (85) Markovitsi, D. Processes triggered in guanine quadruplexes by direct absorption of UV radiation: From fundamental studies toward optoelectronic biosensors. *Photochem. Photobiol.* **2024**, *100* (2), 262–274.
- (86) Miannay, F. A.; Banyasz, A.; Gustavsson, T.; Markovitsi, D. Excited States and Energy Transfer in G-Quadruplexes. *J. Phys. Chem. C* **2009**, *113* (27), 11760–11765.
- (87) Improta, R. Quantum Mechanical Calculations Unveil the Structure and Properties of the Absorbing and Emitting Excited Electronic States of Guanine Quadruplex. *Chem.-Eur. J.* **2014**, *20* (26), 8106–8115.
- (88) Dziuba, D.; Didier, P.; Ciaco, S.; Barth, A.; Seidel, C. A. M.; Mely, Y. Fundamental photophysics of isomeric and expanded fluorescent nucleoside analogues. *Chem. Soc. Rev.* **2021**, *50* (12), 7062–7107.
- (89) Rachwal, P. A.; Fox, K. R. Quadruplex melting. *Methods* **2007**, *43* (4), 291–301.

- (90) Gray, R. D.; Petraccone, L.; Trent, J. O.; Chaires, J. B. Characterization of a K⁺-induced conformational switch in a human telomeric DNA oligonucleotide using 2-aminopurine fluorescence. *Biochemistry* **2010**, *49* (1), 179–94.
- (91) Xu, Y.; Sugiyama, H. Formation of the G-quadruplex and i-motif structures in retinoblastoma susceptibility genes (Rb). *Nucleic Acids Res.* **2006**, *34* (3), 949–54.
- (92) Kimura, T.; Kawai, K.; Fujitsuka, M.; Majima, T. Monitoring G-quadruplex structures and G-quadruplex-ligand complex using 2-aminopurine modified oligonucleotides. *Tetrahedron* **2007**, *63* (17), 3585–3590.
- (93) Nadler, A.; Strohmeier, J.; Diederichsen, U. 8-Vinyl-2'-deoxyguanosine as a Fluorescent 2'-Deoxyguanosine Mimic for Investigating DNA Hybridization and Topology. *Angew. Chem. Int. Edit* **2011**, *50* (23), 5392–5396.
- (94) Ciaco, S.; Gavvala, K.; Greiner, V.; Mazzoleni, V.; Didier, P.; Ruff, M.; Martinez-Fernandez, L.; Improtta, R.; Mely, Y. Thienoguanosine brightness in DNA duplexes is governed by the localization of its ipi* excitation in the lowest energy absorption band. *Methods Appl. Fluoresc* **2022**, *10* (3), 035003.
- (95) Kuchlyan, J.; Martinez-Fernandez, L.; Mori, M.; Gavvala, K.; Ciaco, S.; Boudier, C.; Richert, L.; Didier, P.; Tor, Y.; Improtta, R.; Mely, Y. What Makes Thienoguanosine an Outstanding Fluorescent DNA Probe? *J. Am. Chem. Soc.* **2020**, *142* (40), 16999–17014.
- (96) Ciaco, S.; Mazzoleni, V.; Javed, A.; Eiler, S.; Ruff, M.; Mousli, M.; Mori, M.; Mely, Y. Inhibitors of UHRF1 base flipping activity showing cytotoxicity against cancer cells. *Bioorg. Chem.* **2023**, *137*, No. 106616.
- (97) Sanches de Araujo, A. V.; Valverde, D.; Canuto, S.; Borin, A. C. Solvation Structures and Deactivation Pathways of Luminescent Isothiazole-Derived Nucleobases: (tz)A, (tz)G, and (tz)I. *J. Phys. Chem. A* **2020**, *124* (34), 6834–6844.
- (98) Grytsyk, N.; Richert, L.; Didier, P.; Dziuba, D.; Ciaco, S.; Mazzoleni, V.; Lequeu, T.; Mori, M.; Tor, Y.; Martinez-Fernandez, L.; Improtta, R.; Mely, Y. Thienoguanosine, a unique non-perturbing reporter for investigating rotational dynamics of DNA duplexes and their complexes with proteins. *Int. J. Biol. Macromol.* **2022**, *213*, 210–225.
- (99) Martinez-Fernandez, L.; Gavvala, K.; Sharma, R.; Didier, P.; Richert, L.; Segarra Marti, J.; Mori, M.; Mely, Y.; Improtta, R. Excited-State Dynamics of Thienoguanosine, an Isomorphous Highly Fluorescent Analogue of Guanosine. *Chemistry* **2019**, *25* (30), 7375–7386.
- (100) Sholokh, M.; Improtta, R.; Mori, M.; Sharma, R.; Kenfack, C.; Shin, D.; Voltz, K.; Stote, R. H.; Zaporozhets, O. A.; Botta, M.; Tor, Y.; Mely, Y. Tautomers of a Fluorescent G Surrogate and Their Distinct Photophysics Provide Additional Information Channels. *Angew. Chem., Int. Ed. Engl.* **2016**, *55* (28), 7974–7978.
- (101) Nuthanakanti, A.; Ahmed, I.; Khatik, S. Y.; Saikrishnan, K.; Srivatsan, S. G. Probing G-quadruplex topologies and recognition concurrently in real time and 3D using a dual-app nucleoside probe. *Nucleic Acids Res.* **2019**, *47* (12), 6059–6072.
- (102) Cserenyi, T. Z.; Van Riesen, A. J.; Berger, F. D.; Desoky, A.; Manderville, R. A. A Simple Molecular Rotor for Defining Nucleoside Environment within a DNA Aptamer-Protein Complex. *ACS Chem. Biol.* **2016**, *11* (9), 2576–82.
- (103) Martinez-Fernandez, L.; Esposito, L.; Improtta, R. Studying the excited electronic states of guanine rich DNA quadruplexes by quantum mechanical methods: main achievements and perspectives. *Photochem. Photobiol. Sci.* **2020**, *19* (4), 436–444.
- (104) Balanikas, E.; Martinez-Fernandez, L.; Improtta, R.; Podbevsek, P.; Baldacchino, G.; Markovitsi, D. The Structural Duality of Nucleobases in Guanine Quadruplexes Controls Their Low-Energy Photoionization. *J. Phys. Chem. Lett.* **2021**, *12* (34), 8309–8313.
- (105) Balanikas, E.; Banyasz, A.; Douki, T.; Baldacchino, G.; Markovitsi, D. Guanine Radicals Induced in DNA by Low-Energy Photoionization. *Acc. Chem. Res.* **2020**, *53* (8), 1511–1519.
- (106) Schaffitzel, C.; Berger, I.; Postberg, J.; Hanes, J.; Lipps, H. J.; Pluckthun, A. In vitro generated antibodies specific for telomeric guanine-quadruplex DNA react with *Stylonychia lemnae* macronuclei. *Proc. Natl. Acad. Sci. U. S. A.* **2001**, *98* (15), 8572–7.
- (107) Summers, P. A.; Lewis, B. W.; Gonzalez-Garcia, J.; Porreca, R. M.; Lim, A. H. M.; Cadinu, P.; Martin-Pintado, N.; Mann, D. J.; Edel, J. B.; Vannier, J. B.; Kuimova, M. K.; Vilar, R. Visualising G-quadruplex DNA dynamics in live cells by fluorescence lifetime imaging microscopy. *Nat. Commun.* **2021**, *12*, 162.
- (108) Biffi, G.; Tannahill, D.; McCafferty, J.; Balasubramanian, S. Quantitative visualization of DNA G-quadruplex structures in human cells. *Nat. Chem.* **2013**, *5* (3), 182–6.
- (109) Henderson, A.; Wu, Y.; Huang, Y. C.; Chavez, E. A.; Platt, J.; Johnson, F. B.; Brosh, R. M., Jr.; Sen, D.; Lansdorp, P. M. Detection of G-quadruplex DNA in mammalian cells. *Nucleic Acids Res.* **2017**, *45* (10), 6252.
- (110) Laguerre, A.; Hukezalie, K.; Winckler, P.; Katranji, F.; Chanteloup, G.; Pirrotta, M.; Perrier-Cornet, J. M.; Wong, J. M.; Monchaud, D. Visualization of RNA-Quadruplexes in Live Cells. *J. Am. Chem. Soc.* **2015**, *137* (26), 8521–5.
- (111) Shivalingam, A.; Izquierdo, M. A.; Marois, A. L.; Vysniauskas, A.; Suhling, K.; Kuimova, M. K.; Vilar, R. The interactions between a small molecule and G-quadruplexes are visualized by fluorescence lifetime imaging microscopy. *Nat. Commun.* **2015**, *6*, 8178.
- (112) Xu, H.; Di Antonio, M.; McKinney, S.; Mathew, V.; Ho, B.; O'Neil, N. J.; Santos, N. D.; Silvester, J.; Wei, V.; Garcia, J.; Kabeer, F.; Lai, D.; Soriano, P.; Banath, J.; Chiu, D. S.; Yap, D.; Le, D. D.; Ye, F. B.; Zhang, A.; Thu, K.; Soong, J.; Lin, S. C.; Tsai, A. H.; Osako, T.; Algara, T.; Saunders, D. N.; Wong, J.; Xian, J.; Bally, M. B.; Brenton, J. D.; Brown, G. W.; Shah, S. P.; Cescon, D.; Mak, T. W.; Caldas, C.; Stirling, P. C.; Hieter, P.; Balasubramanian, S.; Aparicio, S. CX-5461 is a DNA G-quadruplex stabilizer with selective lethality in BRCA1/2 deficient tumours. *Nat. Commun.* **2017**, *8*, No. 14432.
- (113) Jin, M.; Hurley, L. H.; Xu, H. A synthetic lethal approach to drug targeting of G-quadruplexes based on CX-5461. *Bioorg. Med. Chem. Lett.* **2023**, *91*, No. 129384.
- (114) Xu, H.; Hurley, L. H. A first-in-class clinical G-quadruplex-targeting drug. The bench-to bedside translation of the fluoroquinolone QQ58 to CX-5461 (Pidnarulex). *Bioorg. Med. Chem. Lett.* **2022**, *77*, No. 129016.
- (115) Drygin, D.; Siddiqui-Jain, A.; O'Brien, S.; Schwaebel, M.; Lin, A.; Bliesath, J.; Ho, C. B.; Proffitt, C.; Trent, K.; Whitten, J. P.; Lim, J. K.; Von Hoff, D.; Anderes, K.; Rice, W. G. Anticancer activity of CX-3543: a direct inhibitor of rRNA biogenesis. *Cancer Res.* **2009**, *69* (19), 7653–61.
- (116) Ahmed, A. A.; Angell, R.; Oxenford, S.; Worthington, J.; Williams, N.; Barton, N.; Fowler, T. G.; O'Flynn, D. E.; Sunose, M.; McConville, M.; Vo, T.; Wilson, W. D.; Karim, S. A.; Morton, J. P.; Neidle, S. Asymmetrically Substituted Quadruplex-Binding Naphthalene Diimide Showing Potent Activity in Pancreatic Cancer Models. *ACS Med. Chem. Lett.* **2020**, *11* (8), 1634–1644.
- (117) Rawal, P.; Kummarasetti, V. B.; Ravindran, J.; Kumar, N.; Halder, K.; Sharma, R.; Mukerji, M.; Das, S. K.; Chowdhury, S. Genome-wide prediction of G4 DNA as regulatory motifs: role in *Escherichia coli* global regulation. *Genome Res.* **2006**, *16* (5), 644–55.
- (118) Vogt, R. L.; Dippold, L. *Escherichia coli* O157:H7 outbreak associated with consumption of ground beef, June–July 2002. *Public Health Rep* **2005**, *120* (2), 174–8.
- (119) Holder, I. T.; Hartig, J. S. A matter of location: influence of G-quadruplexes on *Escherichia coli* gene expression. *Chem. Biol.* **2014**, *21* (11), 1511–21.
- (120) Takenaka, S. Application of naphthalene diimide in biotechnology. *Polym. J.* **2021**, *53* (3), 415–427.
- (121) Al Kobaisi, M.; Bhosale, S. V.; Latham, K.; Raynor, A. M.; Bhosale, S. V. Functional Naphthalene Diimides: Synthesis, Properties, and Applications. *Chem. Rev.* **2016**, *116* (19), 11685–11796.
- (122) Bhosale, S. V.; Al Kobaisi, M.; Jadhav, R. W.; Morajkar, P. P.; Jones, L. A.; George, S. Naphthalene diimides: perspectives and promise. *Chem. Soc. Rev.* **2021**, *50* (17), 9845–9998.

- (123) Pirola, V.; Nadai, M.; Doria, F.; Richter, S. N. Naphthalene Diimides as Multimodal G-Quadruplex-Selective Ligands. *Molecules* **2019**, *24* (3), 426.
- (124) Cebrian, R.; Belmonte-Reche, E.; Pirola, V.; de Jong, A.; Morales, J. C.; Freccero, M.; Doria, F.; Kuipers, O. P. G-Quadruplex DNA as a Target in Pathogenic Bacteria: Efficacy of an Extended Naphthalene Diimide Ligand and Its Mode of Action. *J. Med. Chem.* **2022**, *65* (6), 4752–4766.
- (125) Ahmed, A. A.; Chen, S.; Roman-Escorza, M.; Angell, R.; Oxenford, S.; McConville, M.; Barton, N.; Sunose, M.; Neidle, D.; Haider, S.; Arshad, T.; Neidle, S. Structure-activity relationships for the G-quadruplex-targeting experimental drug QN-302 and two analogues probed with comparative transcriptome profiling and molecular modeling. *Sci. Rep.* **2024**, *14*, 3447.
- (126) Belmonte-Reche, E.; Morales, J. C. G4-iM Grinder: when size and frequency matter. G-Quadruplex, i-Motif and higher order structure search and analysis tool. *NAR Genom Bioinform* **2020**, *2* (1), No. lqz005.
- (127) Takebayashi, Y.; Ramos-Soriano, J.; Jiang, Y. J.; Samphire, J.; Belmonte-Reche, E.; O'Hagan, M. P.; Gurr, C.; Heesom, K. J.; Lewis, P. A.; Samernate, T.; Nonejuie, P.; Spencer, J.; Galan, M. C. Small molecule G-quadruplex ligands are antibacterial candidates for Gram-negative bacteria. *bioRxiv* **2024**, DOI: 10.1101/2022.09.01.506212.
- (128) Koirala, D.; Dhakal, S.; Ashbridge, B.; Sannohe, Y.; Rodriguez, R.; Sugiyama, H.; Balasubramanian, S.; Mao, H. A single-molecule platform for investigation of interactions between G-quadruplexes and small-molecule ligands. *Nat. Chem.* **2011**, *3* (10), 782–7.
- (129) Siddiqui-Jain, A.; Grand, C. L.; Bearss, D. J.; Hurley, L. H. Direct evidence for a G-quadruplex in a promoter region and its targeting with a small molecule to repress c-MYC transcription. *Proc. Natl. Acad. Sci. U. S. A.* **2002**, *99* (18), 11593–8.
- (130) Mikami-Terao, Y.; Akiyama, M.; Yuza, Y.; Yanagisawa, T.; Yamada, O.; Yamada, H. Antitumor activity of G-quadruplex-interactive agent TMPyP4 in K562 leukemic cells. *Cancer Lett.* **2008**, *261* (2), 226–34.
- (131) Onel, B.; Carver, M.; Wu, G.; Timonina, D.; Kalarn, S.; Larriva, M.; Yang, D. A New G-Quadruplex with Hairpin Loop Immediately Upstream of the Human BCL2 P1 Promoter Modulates Transcription. *J. Am. Chem. Soc.* **2016**, *138* (8), 2563–70.
- (132) Cogoi, S.; Xodo, L. E. G-quadruplex formation within the promoter of the proto-oncogene and its effect on transcription. *Nucleic Acids Res.* **2006**, *34* (9), 2536–2549.
- (133) Zhou, G.; Liu, X.; Li, Y.; Xu, S.; Ma, C.; Wu, X.; Cheng, Y.; Yu, Z.; Zhao, G.; Chen, Y. Telomere targeting with a novel G-quadruplex-interactive ligand BRACO-19 induces T-loop disassembly and telomerase displacement in human glioblastoma cells. *Oncotarget* **2016**, *7* (12), 14925–39.
- (134) Perrone, R.; Butovskaya, E.; Daelemans, D.; Palu, G.; Pannecoque, C.; Richter, S. N. Anti-HIV-1 activity of the G-quadruplex ligand BRACO-19. *J. Antimicrob. Chemother.* **2014**, *69* (12), 3248–58.
- (135) Burger, A. M.; Dai, F.; Schultes, C. M.; Reszka, A. P.; Moore, M. J.; Double, J. A.; Neidle, S. The G-quadruplex-interactive molecule BRACO-19 inhibits tumor growth, consistent with telomere targeting and interference with telomerase function. *Cancer Res.* **2005**, *65* (4), 1489–96.
- (136) Stempel, N.; Neidig, A.; Nusser, M.; Geffers, R.; Vieillard, J.; Lesouhaitier, O.; Brenner-Weiss, G.; Overhage, J. Human host defense peptide LL-37 stimulates virulence factor production and adaptive resistance in *Pseudomonas aeruginosa*. *PLoS One* **2013**, *8* (12), No. e82240.
- (137) Jackson, K. D.; Starkey, M.; Kremer, S.; Parsek, M. R.; Wozniak, D. J. Identification of psl, a locus encoding a potential exopolysaccharide that is essential for *Pseudomonas aeruginosa* PAO1 biofilm formation. *J. Bacteriol.* **2004**, *186* (14), 4466–75.
- (138) Ryder, C.; Byrd, M.; Wozniak, D. J. Role of polysaccharides in *Pseudomonas aeruginosa* biofilm development. *Curr. Opin Microbiol* **2007**, *10* (6), 644–8.
- (139) Ghafoor, A.; Hay, I. D.; Rehm, B. H. Role of exopolysaccharides in *Pseudomonas aeruginosa* biofilm formation and architecture. *Appl. Environ. Microbiol.* **2011**, *77* (15), 5238–46.
- (140) Xuan, T. F.; Wang, Z. Q.; Liu, J.; Yu, H. T.; Lin, Q. W.; Chen, W. M.; Lin, J. Design and Synthesis of Novel c-di-GMP G-Quadruplex Inducers as Bacterial Biofilm Inhibitors. *J. Med. Chem.* **2021**, *64* (15), 11074–11089.
- (141) Neidle, S. Quadruplex Nucleic Acids as Novel Therapeutic Targets. *J. Med. Chem.* **2016**, *59* (13), 5987–6011.
- (142) Seviour, T.; Winnerdy, F. R.; Wong, L. L.; Shi, X. Y.; Mugunthan, S.; Foo, Y. H.; Castaing, R.; Adav, S. S.; Subramoni, S.; Kohli, G. S.; Shewan, H. M.; Stokes, J. R.; Rice, S. A.; Phan, A. T.; Kjelleberg, S. The biofilm matrix scaffold of contains G-quadruplex extracellular DNA structures. *npj Biofilms Microbi.* **2021**, *7*, 27.
- (143) Evans, L.; Kotar, A.; Valentini, M.; Filloux, A.; Jamshidi, S.; Plavec, J.; Rahman, K. M.; Vilar, R. Identification and characterisation of G-quadruplex DNA-forming sequences in the *Pseudomonas aeruginosa* genome. *RSC Chem. Biol.* **2023**, *4* (1), 94–100.
- (144) Kikin, O.; D'Antonio, L.; Bagga, P. S. QGRS Mapper: a web-based server for predicting G-quadruplexes in nucleotide sequences. *Nucleic Acids Res.* **2006**, *34*, W676.
- (145) Cahoon, L. A.; Seifert, H. S. An Alternative DNA Structure Is Necessary for Pilin Antigenic Variation in *Neisseria gonorrhoeae*. *Science* **2009**, *325* (5941), 764–767.
- (146) Cahoon, L. A.; Seifert, H. S. Transcription of a cis-acting, Noncoding, Small RNA Is Required for Pilin Antigenic Variation in *Neisseria gonorrhoeae*. *PLoS Pathog.* **2013**, *9* (1), No. e1003074.
- (147) Robertson, J. N.; Vincent, P.; Ward, M. E. The preparation and properties of gonococcal pili. *J. Gen. Microbiol.* **1977**, *102* (1), 169–77.
- (148) Lauer, P.; Albertson, N. H.; Koomey, M. Conservation of genes encoding components of a type IV pilus assembly/two-step protein export pathway in *Neisseria gonorrhoeae*. *Mol. Microbiol.* **1993**, *8* (2), 357–68.
- (149) Cohen, M. S.; Cannon, J. G. Human experimentation with *Neisseria gonorrhoeae*: progress and goals. *J. Infect Dis* **1999**, *179*, S375.
- (150) Prister, L. L.; Yin, S.; Cahoon, L. A.; Seifert, H. S. Altering the *Neisseria gonorrhoeae* pilE Guanine Quadruplex Loop Bases Affects Pilin Antigenic Variation. *Biochemistry* **2020**, *59* (10), 1104–1112.
- (151) Voter, A. F.; Callaghan, M. M.; Tippiana, R.; Myong, S.; Dillard, J. P.; Keck, J. L. Antigenic Variation in *Neisseria gonorrhoeae* Occurs Independently of RecQ-Mediated Unwinding of the pilE G Quadruplex. *J. Bacteriol.* **2020**, DOI: 10.1128/JB.00607-19.
- (152) Rotman, E.; Seifert, H. S. The genetics of *Neisseria* species. *Annu. Rev. Genet.* **2014**, *48*, 405–31.
- (153) Walia, R.; Chaconas, G. Suggested Role for G4 DNA in Recombinational Switching at the Antigenic Variation Locus of the Lyme Disease Spirochete. *PLoS One* **2013**, *8* (2), e57792.
- (154) Giacani, L.; Brandt, S. L.; Puray-Chavez, M.; Reid, T. B.; Godornes, C.; Molini, B. J.; Benzler, M.; Hartig, J. S.; Lukehart, S. A.; Centurion-Lara, A. Comparative Investigation of the Genomic Regions Involved in Antigenic Variation of the TprK Antigen among Treponemal Species, Subspecies, and Strains. *J. Bacteriol.* **2012**, *194* (16), 4208–4225.
- (155) Glover, L.; Alsford, S.; Horn, D. DNA Break Site at Fragile Subtelomeres Determines Probability and Mechanism of Antigenic Variation in African Trypanosomes. *PLoS Pathog* **2013**, *9* (3), No. e1003260.
- (156) Smargiasso, N.; Gabelica, V.; Damblon, C.; Rosu, F.; De Pauw, E.; Teulade-Fichou, M. P.; Rowe, J. A.; Claessens, A. Putative DNA G-quadruplex formation within the promoters of genes. *BMC Genomics* **2009**, *10*, 362.
- (157) Mishra, S. K.; Tawani, A.; Mishra, A.; Kumar, A. G4IPDB: A database for G-quadruplex structure forming nucleic acid interacting proteins. *Sci. Rep.* **2016**, *6*, 38144.
- (158) Jain, N.; Shankar, U.; Singh, A.; Sharma, T. K.; Kumar, A. G-quadruplex motifs in *Neisseria gonorrhoeae* as anti-gonococcal targets. *Appl. Microbiol. Biotechnol.* **2023**, *107* (16), 5145–5159.

- (159) Dai, J.; Chen, D.; Jones, R. A.; Hurley, L. H.; Yang, D. NMR solution structure of the major G-quadruplex structure formed in the human BCL2 promoter region. *Nucleic Acids Res.* **2006**, *34* (18), 5133–44.
- (160) Global Tuberculosis Programme. *WHO Global tuberculosis report 2023*; World Health Organization: Geneva, Switzerland, 2023. <https://www.who.int/publications/i/item/9789240083851> (accessed 2024-02-15).
- (161) Keane, J.; Balcewicz-Sablinska, M. K.; Remold, H. G.; Chupp, G. L.; Meek, B. B.; Fenton, M. J.; Kornfeld, H. Infection by *Mycobacterium tuberculosis* promotes human alveolar macrophage apoptosis. *Infect. Immun.* **1997**, *65* (1), 298–304.
- (162) Hunter, R. L.; Olsen, M. R.; Jagannath, C.; Actor, J. K. Multiple roles of cord factor in the pathogenesis of primary, secondary, and cavitory tuberculosis, including a revised description of the pathology of secondary disease. *Ann. Clin Lab Sci.* **2006**, *36* (4), 371–386.
- (163) Mann, F. M.; Xu, M.; Chen, X.; Fulton, D. B.; Russell, D. G.; Peters, R. J. Edaxadiene: a new bioactive diterpene from *Mycobacterium tuberculosis*. *J. Am. Chem. Soc.* **2009**, *131* (48), 17526–7.
- (164) Flynn, J. L.; Chan, J. Immune evasion by *Mycobacterium tuberculosis*: living with the enemy. *Curr. Opin Immunol* **2003**, *15* (4), 450–5.
- (165) Buter, J.; Cheng, T. Y.; Ghanem, M.; Grootemaat, A. E.; Raman, S.; Feng, X.; Plantijn, A. R.; Ennis, T.; Wang, J.; Cotton, R. N.; Layre, E.; Ramnarine, A. K.; Mayfield, J. A.; Young, D. C.; Jezek Martinot, A.; Siddiqi, N.; Wakabayashi, S.; Botella, H.; Calderon, R.; Murray, M.; Ehrst, S.; Snider, B. B.; Reed, M. B.; Oldfield, E.; Tan, S.; Rubin, E. J.; Behr, M. A.; van der Wel, N. N.; Minnaard, A. J.; Moody, D. B. *Mycobacterium tuberculosis* releases an antacid that remodels phagosomes. *Nat. Chem. Biol.* **2019**, *15* (9), 889–899.
- (166) Brodin, P.; Hoffmann, E. T(oo)bAd. *Nat. Chem. Biol.* **2019**, *15* (9), 849–850.
- (167) Cohen, S. B.; Gern, B. H.; Urdahl, K. B. The Tuberculous Granuloma and Preexisting Immunity. *Annu. Rev. Immunol.* **2022**, *40*, 589–614.
- (168) Perrone, R.; Lavezzo, E.; Riello, E.; Manganelli, R.; Palu, G.; Toppo, S.; Proveddi, R.; Richter, S. N. Mapping and characterization of G-quadruplexes in *Mycobacterium tuberculosis* gene promoter regions. *Sci. Rep* **2017**, *7*, 5743.
- (169) Dey, A.; Anand, K.; Singh, A.; Prasad, R.; Barthwal, R. Binding-induced thermal stabilization of *mosR* and *ndhA* G-quadruplex comprising genes by emodin leads to downregulation and growth inhibition in *Mtb*: Potential as anti-tuberculosis drug. *Results Chem.* **2023**, *6*, 101114.
- (170) Dey, A.; Anand, K.; Singh, A.; Prasad, R.; Barthwal, R. MOSR and NDHA Genes Comprising G-Quadruplex as Promising Therapeutic Targets against *Mycobacterium tuberculosis*: Molecular Recognition by Mitoxantrone Suppresses Replication and Gene Regulation. *Genes* **2023**, *14* (5), 978.
- (171) Mishra, S. K.; Shankar, U.; Jain, N.; Sikri, K.; Tyagi, J. S.; Sharma, T. K.; Mergny, J. L.; Kumar, A. Characterization of G-Quadruplex Motifs in *espB*, *espK*, and *cyp51* Genes of *Mycobacterium tuberculosis* as Potential Drug Targets. *Mol. Ther Nucleic Acids* **2019**, *16*, 698–706.
- (172) van de Beek, D.; de Gans, J.; Tunkel, A. R.; Wijdicks, E. F. Community-acquired bacterial meningitis in adults. *N Engl J. Med.* **2006**, *354* (1), 44–53.
- (173) Koedel, U.; Scheld, W. M.; Pfister, H. W. Pathogenesis and pathophysiology of pneumococcal meningitis. *Lancet Infect Dis* **2002**, *2* (12), 721–36.
- (174) Mishra, S. K.; Jain, N.; Shankar, U.; Tawani, A.; Sharma, T. K.; Kumar, A. Characterization of highly conserved G-quadruplex motifs as potential drug targets in *Streptococcus pneumoniae*. *Sci. Rep* **2019**, *9*, 1791.
- (175) Carmichael, A. G. *Plagues in World History*. By John Aberth (Lanham, Md., Rowman Littlefield, 2011) 243 pp. \$34.95. *Journal of Interdisciplinary History* **2012**, *43* (1), 77–78.
- (176) Yoon, S. H.; Waters, C. M. *Vibrio cholerae*. *Trends Microbiol* **2019**, *27* (9), 806–807.
- (177) Verma, J.; Bag, S.; Saha, B.; Kumar, P.; Ghosh, T. S.; Dayal, M.; Senapati, T.; Mehra, S.; Dey, P.; Desigamani, A.; Kumar, D.; Rana, P.; Kumar, B.; Maiti, T. K.; Sharma, N. C.; Bhadra, R. K.; Mutreja, A.; Nair, G. B.; Ramamurthy, T.; Das, B. Genomic plasticity associated with antimicrobial resistance in *Vibrio cholerae*. *Proc. Natl. Acad. Sci. U. S. A.* **2019**, *116* (13), 6226–6231.
- (178) Kitaoka, M.; Miyata, S. T.; Unterweger, D.; Pukatzki, S. Antibiotic resistance mechanisms of *Vibrio cholerae*. *J. Med. Microbiol* **2011**, *60*, 397–407.
- (179) Shankar, U.; Jain, N.; Majee, P.; Kodgire, P.; Sharma, T. K.; Kumar, A. Exploring Computational and Biophysical Tools to Study the Presence of G-Quadruplex Structures: A Promising Therapeutic Solution for Drug-Resistant *Vibrio cholerae*. *Front. Genet.* **2020**, *11*, 935.
- (180) Lin, W.; Fullner, K. J.; Clayton, R.; Sexton, J. A.; Rogers, M. B.; Calia, K. E.; Calderwood, S. B.; Fraser, C.; Mekalanos, J. J. Identification of a *vibrio cholerae* RTX toxin gene cluster that is tightly linked to the cholera toxin prophage. *Proc. Natl. Acad. Sci. U. S. A.* **1999**, *96* (3), 1071–6.
- (181) Paczosa, M. K.; Meccas, J. *Klebsiella pneumoniae*: Going on the Offense with a Strong Defense. *Microbiol Mol. Biol. Rev.* **2016**, *80* (3), 629–61.
- (182) Sanchez-Lopez, J.; Garcia-Caballero, A.; Navarro-San Francisco, C.; Quereda, C.; Ruiz-Garbajosa, P.; Navas, E.; Dronda, F.; Morosini, M. I.; Canton, R.; Diez-Aguilar, M. Hypermucoviscous *Klebsiella pneumoniae*: A challenge in community acquired infection. *IDCases* **2019**, *17*, No. e00547.
- (183) Shankar, U.; Jain, N.; Mishra, S. K.; Sharma, T. K.; Kumar, A. Conserved G-Quadruplex Motifs in Gene Promoter Region Reveals a Novel Therapeutic Approach to Target Multi-Drug Resistance *Klebsiella pneumoniae*. *Front. Microbiol.* **2020**, *11*, 1269.
- (184) Backert, S.; Neddermann, M.; Maubach, G.; Naumann, M. Pathogenesis of *Helicobacter pylori* infection. *Helicobacter* **2016**, *21*, 19–25.
- (185) Domanovich-Asor, T.; Craddock, H. A.; Motro, Y.; Khalfin, B.; Peretz, A.; Moran-Gilad, J. Unraveling antimicrobial resistance in *Helicobacter pylori*: Global resistome meets global phylogeny. *Helicobacter* **2021**, *26* (2), No. e12782.
- (186) Shankar, U.; Mishra, S. K.; Jain, N.; Tawani, A.; Yadav, P.; Kumar, A. Ni(+2) permease system of *Helicobacter pylori* contains highly conserved G-quadruplex motifs. *Infect Genet Evol* **2022**, *101*, No. 105298.
- (187) de Reuse, H.; Vinella, D.; Cavazza, C. Common themes and unique proteins for the uptake and trafficking of nickel, a metal essential for the virulence of *Helicobacter pylori*. *Front. Cell Infect. Microbiol.* **2013**, *3*, 94.
- (188) Lipinski, C. A.; Lombardo, F.; Dominy, B. W.; Feeney, P. J. Experimental and computational approaches to estimate solubility and permeability in drug discovery and development settings. *Adv. Drug Deliv Rev.* **2001**, *46* (1–3), 3–26.
- (189) Collie, G.; Reszka, A. P.; Haider, S. M.; Gabelica, V.; Parkinson, G. N.; Neidle, S. Selectivity in small molecule binding to human telomeric RNA and DNA quadruplexes. *Chem. Commun. (Camb)* **2009**, No. 48, 7482–4.
- (190) Zuffo, M.; Guedin, A.; Leriche, E. D.; Doria, F.; Pirotta, V.; Gabelica, V.; Mergny, J. L.; Freccero, M. More is not always better: finding the right trade-off between affinity and selectivity of a G-quadruplex ligand. *Nucleic Acids Res.* **2018**, *46* (19), No. e115.
- (191) Frasson, I.; Nadai, M.; Richter, S. N. Conserved G-Quadruplexes Regulate the Immediate Early Promoters of Human Alphaherpesviruses. *Molecules* **2019**, *24* (13), 2375.
- (192) Cosconati, S.; Marinelli, L.; Trotta, R.; Virno, A.; De Tito, S.; Romagnoli, R.; Pagano, B.; Limongelli, V.; Giancola, C.; Baraldi, P. G.; Mayol, L.; Novellino, E.; Randazzo, A. Structural and conformational requisites in DNA quadruplex groove binding: another piece to the puzzle. *J. Am. Chem. Soc.* **2010**, *132* (18), 6425–33.

(193) Scott, L.; Chalikian, T. V. Stabilization of G-Quadruplex-Duplex Hybrid Structures Induced by Minor Groove-Binding Drugs. *Life* **2022**, *12* (4), 597.

(194) Halder, D.; Purkayastha, P. A flavonol that acts as a potential DNA minor groove binder as also an efficient G-quadruplex loop binder. *J. Mol. Liq.* **2018**, *265*, 69–76.

(195) Platella, C.; Ghirga, F.; Musumeci, D.; Quaglio, D.; Zizza, P.; Iachettini, S.; D'Angelo, C.; Biroccio, A.; Botta, B.; Mori, M.; Montesarchio, D. Selective Targeting of Cancer-Related G-Quadruplex Structures by the Natural Compound Dicentrine. *Int. J. Mol. Sci.* **2023**, *24* (4), 4070.

(196) Platella, C.; Ghirga, F.; Zizza, P.; Pompili, L.; Marzano, S.; Pagano, B.; Quaglio, D.; Vergine, V.; Cammarone, S.; Botta, B.; Biroccio, A.; Mori, M.; Montesarchio, D. Identification of Effective Anticancer G-Quadruplex-Targeting Chemotypes through the Exploration of a High Diversity Library of Natural Compounds. *Pharmaceutics* **2021**, *13* (10), 1611.

(197) Di Leva, F. S.; Zizza, P.; Cingolani, C.; D'Angelo, C.; Pagano, B.; Amato, J.; Salvati, E.; Sissi, C.; Pinato, O.; Marinelli, L.; Cavalli, A.; Cosconati, S.; Novellino, E.; Randazzo, A.; Biroccio, A. Exploring the chemical space of G-quadruplex binders: discovery of a novel chemotype targeting the human telomeric sequence. *J. Med. Chem.* **2013**, *56* (23), 9646–54.

(198) Cosconati, S.; Marinelli, L.; Trotta, R.; Virno, A.; Mayol, L.; Novellino, E.; Olson, A. J.; Randazzo, A. Tandem application of virtual screening and NMR experiments in the discovery of brand new DNA quadruplex groove binders. *J. Am. Chem. Soc.* **2009**, *131* (45), 16336–7.